MIT - 2073 - 8
MITNE - 89

MASSACHUSETTS INSTITUTE OF TECHNOLOGY
DEPARTMENT OF NUCLEAR ENGINEERING
Cambridge, Massachusetts 02139

SUMMARY DESCRIPTION OF THE FUEL DEPLETION CODE, CELL

by

D. A. Goellner and J. J. Beaudreau

June 1968

For the
U.S. Atomic Energy Commission
Under Contract AT(30-1) - 2073

MIT-2073-8
MITNE-89

MASSACHUSETTS INSTITUTE OF TECHNOLOGY
DEPARTMENT OF NUCLEAR ENGINEERING

Summary Description of the Fuel Depletion Code, CELL

D. A. Goellner and J. J. Beaudreau

June 30, 1968

For United States Atomic Energy Commission
Contract AT(30-1)-2073

ABSTRACT

The CELL code performs a modified-two group, point-depletion calculation and determines the characteristics of a unit reactor cell as functions of thermal flux-time. These characteristics are prepared by CELL in a form suitable for use by the fuel management code MOVE, which carries out reactivity and spatial flux calculations throughout core life and simulates various refueling schemes.

Using the earlier FUEL code as a starting point, CELL was developed to provide a means for accurately predicting the fuel cycle performance of light-water-moderated reactors, while retaining a level of sophistication consistent with the requirement of low computer time usage and without introducing any changes to MOVE.

The major differences between the CELL and FUEL codes are discussed, and a comparison is made of the accuracy with which the two codes predict the experimentally-determined variations of fuel isotopic composition with burnup for the Yankee Reactor. First cycle characteristics predicted by CELL-MOVE for the San Onofre pressurized-water reactor are compared with Westinghouse calculations. Conclusions are drawn concerning the ability of CELL to accurately predict PWR fuel cycle characteristics.

The theory and assumptions included in CELL are discussed in sufficient detail to enable the reader to judge the applicability of the code to particular reactor types and problems. All principal equations are given and a broad logical flow diagram of the code is presented.

TABLE OF CONTENTS

LIST OF FIGURES

LIST OF TABLES

I. INTRODUCTION

A. Background

The fuel management code FUELCYC (1), written at M.I.T. by R. T. Shanstrom, has served as the precursor of several other codes similar in scope but incorporating refinements in the calculational models or changes of a problem-oriented nature. Chief among these codes based on Shanstrom's work is FUELMOVE (2), developed at M.I.T. by N. B. McLeod. FUELMOVE retains the basic two-dimensional, modified two group calculation of FUELCYC but utilizes an improved version of the FUELCYC neutron behavior model and also provides a wider choice of schemes for reloading and shuffling fuel than does the older code. Both FUELMOVE and FUELCYC are designed for use in survey work, rather than for detailed design calculations. Their major advantage is that they can be used to determine the fuel burnup and gross power shapes for a large number of fuel and poison management techniques with a minimum expenditure of computer time, a characteristic not found in the reactor depletion codes usually used for detailed design work. The saving in computation time results primarily from the use of coarse mesh spacings in the flux and power distribution calculations and from the calculation of fuel burnup on a flux-time basis rather than with point-by-point depletion. Due to their inability to predict fine-structure in the power distribution, the application of the codes has been limited to studies of the relative desirability of various fuel and poison management schemes and the relative importance of the broad trends they exhibit. In keeping with this general purpose, the degree of approximation in FUELCYC and FUELMOVE is quite high, and model sophistication is kept at a level which does not affect the basic requirement of minimum computer time.

For convenience and increased efficiency, the FUELMOVE code was written as two separate codes - FUEL and MOVE. In

the FUEL code, the flux-time dependence of nuclide concentrations and lattice properties is computed for a specified type and enrichment of fuel. This information plus geometrical data for the given reactor is subsequently used by the MOVE code, which computes spatial flux shapes and power densities during fuel irradiation, obtains the discharged fuel properties and burnup, and computes fuel cycle and total energy cost for a specified combination of the fuel and poison management techniques which are written into the code. The MOVE code also has the capability to simulate the refueling of the given reactor a sufficient number of times to reach the steady-state operating condition for the particular fuel material and management schemes selected.

McLeod (2) found that FUELMOVE has the capability of predicting, with good accuracy, many of the experimentally-determined time-dependent characteristics of heavy-water reactors. Subsequent efforts by Menezes (3) to use FUELMOVE in predicting the fuel cycle performance of the first core of the Yankee reactor were less usccessful, and it was apparent that the approximations used in FUELMOVE are less valid for light-water reactors than for heavy-water reactors. However, comparison of Yankee experimental results with FUELMOVE results indicated that discrepancies might be lessened by modifying the treatment of resonance reactions in FUEL and by re-evaluating the built-in library of nuclear data. Thus, the original version of FUELMOVE was judged inadequate for accurate prediction of pressurized-light-water reactor (PWR) characteristics, but improvement appeared possible by suitable revision of the code.

B. Objectives

A strong incentive for improving the ability of the FUELMOVE code to accurately treat PWR systems was provided by the computational requirements of D. A. Goellner (4) in his study of the effect of isotopic composition on the value of uranium

used as makeup feed for PWR fuel cycles. Goellner's work uses the 430 MWe San Onofre Reactor as a reference PWR. This study necessitated the performance of numerous depletion calculations, with particular emphasis on the accurate prediction of U-235 and U-236 concentrations throughout each irradiation cycle in order to obtain meaningful results.

Although a number of codes were considered by Goellner, FUELMOVE, with its small computer time requirement, appeared the best choice for the study from a practical viewpoint, provided its accuracy in predicting Yankee characteristics could be improved to an acceptable level. In particular, increased accuracy in predicting U-235 and U-236 concentrations was mandatory, and it was hoped that discharged fuel burnup could be shown to be accurate within 10% of the correct value. Also desirable, though less important for Goellner's study, was an improvement in the prediction of fissile plutonium content in discharged fuel. It was desired that these goals be attained by revision of the FUEL code so that the resulting code would retain the twin virtues of speed and simplicity and remain completely compatible with the original version of the MOVE code.

The task of revising FUEL was undertaken by J. J. Beaudreau at M.I.T. as a Master's Degree thesis (5). The result of Beaudreau's work was a new code, CELL, the performance and description of which are summarized in this volume.

C. Brief Comparison of CELL and FUEL

The CELL code retains the basic philosophy of the FUEL code, which assumes that the unit reactor cell can be effectively represented by a volume- and flux-weighted homogenized equivalent and that the nuclide concentrations and unit cell properties can be represented as functions of only one variable -- thermal flux-time. As in FUEL, this information is transferred by tape or cards to the MOVE code, which determines the spatial dependence of both thermal flux and fuel composition throughout the core irradiation. The neutron cycle

used in CELL is also similar to that in FUEL, as is the handling of fission products, but the methods used to treat both the thermal and resonance groups differ in many respects. The input data specification and the division of various calculations between the main program and subroutines are considerably different for CELL, although the functions of most subroutines common to both codes remain the same as in FUEL.

Table I.1 summarizes the most significant differences between the CELL and FUEL codes. Both codes permit the calculation of a thermal neutron energy distribution according to the Wilkins heavy gas model (6), but an important inclusion in CELL is the provision for calculating a thermal spectrum using the Wigner-Wilkins hydrogen model (7) as an alternative to the Wilkins model. The Wigner-Wilkins model has been widely used in calculating spectrum-averaged thermal constants for PWR's (8,9).

The treatment of thermal disadvantage factors in CELL represents a drastic departure in both convenience and sophistication from that in FUEL, where a single, energy-independent value for the ratio of average thermal flux in all non-fuel materials to the average thermal flux in the fuel is required as input. In CELL, energy-dependent thermal flux disadvantage factors are calculated for fuel (meat), cladding, coolant, and "extra" (nonlattice) regions, with only geometric and microscopic cross-section data required as input. The average thermal flux in the unit cell is used as the basis for normalization in CELL, whereas the average thermal flux in the fuel is used in FUEL.

Microscopic absorption and fission cross-sections for fuel nuclides are calculated by FUEL at each energy point in the thermal region using the formulation developed by Westcott (10); however, CELL requires that these cross-sections be read in as input, thereby providing flexibility in the choice of microscopic data at the expense of additional card-handling

TABLE I.1 Major Differences Between CELL and FUEL

Item	CELL Treatment	FUEL Treatment
Thermal spectrum	Wilkins or Wigner-Wilkins	Wilkins
Thermal disadvantage factors	Energy- and time-dependent; calculated by code separately for fuel, clad, coolant, and "extra" (nonlattice) regions; normalized to average flux in cell	Energy- and time-dependent; one factor averaged over all nonfuel regions is read in; normalized to average flux in fuel
Effective resonance integrals (except U-238)	Numerical integration down to thermal cutoff energy	Crowther-Weil
U-238 resonance integral	Input, or calculated with dependence on time and fuel temperature	Input value held constant during cycle
U-235 resonance integral	Provision for adjusting calculated values; absorption and fission integrals calculated separately	No adjustment possible; fission integral found from calculated absorption integral and constant resonance α
Thermal point cross-sections	Input	Calculated from Westcott formulation
Np-237 concentration	Calculated	Not calculated

and data preparation, the latter being incurred only once for all CELL cases based on the same source of microscopic data.

The rather crude Crowther-Weil (11) treatment of effective resonance integrals for fuel nuclides (except for U-238) has been replaced in CELL by numerical integration of an equation for the effective resonance integral (see Section III.B.4). This latter procedure requires that a library of resonance cross-sections as functions of energy be read in as input, but the calculation is put on a firmer theoretical basis.

The resonance integral for U-238, required as a time-dependent input value by FUEL, can be calculated at each point in time by CELL using a reliable empirical expression which includes the effect of average fuel temperature.

CELL allows for the time variation of the capture-to-fission ratio for U-235 in the resonance region by recalculating effective resonance integrals for both absorption and fission at each time step. FUEL, on the other hand, calculates a time-dependent absorption resonance integral for U-235 but uses a constant capture-to-fission ratio to obtain the fission resonance integral. The importance of U-235 resonance reactions in typical light-water-moderated reactors is considerable, and slight errors in predicting U-235 resonance integrals can lead to significant errors in predicting core lifetime and discharge fuel composition; hence, a provision for separate adjustment of the U-235 absorption and fission integrals by reading in time-independent adjustment factors was incorporated into CELL. It was expected that the degree of adjustment necessary to obtain satisfactory results would be about the same for all practical PWR designs and that these adjustment factors would require "tuning" only once.

The calculation of Np-237 number density is not carried out by FUEL but was added to the chain of nuclides in CELL as an obvious requirement of Goellner's study (4).

Many other differences of lesser significance exist between CELL and FUEL. These are described in considerable de-

tail by Beaudreau (5), who presents a separate evaluation of each modification to FUEL which lead to the final CELL version. The interested reader is also referred to Beaudreau's work for details of input preparation for CELL, descriptions of subroutines, and a complete FORTRAN listing of the CELL code.

II. PREDICTION OF PWR CHARACTERISTICS

A. Cases Considered

The major objective in developing the CELL code was to predict the fuel cycle performance of light water reactors accurately. Consequently, a comparison between the results of CELL and the experimental data from the first and second cores of the Yankee Reactor was used throughout the development of the code to check its accuracy. The dangers inherent in evaluating accuracy based on a single set of reactor characteristics is obvious; hence, it was felt that the code should be used to compute the performance of a second light-water reactor whose characteristics were known to a high degree of accuracy. Since Goellner's work (4) was to be based on a reactor having the properties of the San Onofre Reactor, it was decided to use that reactor as a second basis for evaluation. In this case, comparison is made with the Westinghouse reference design calculations (12) as experimental data are not yet available.

The usefulness of Yankee data in evaluating CELL was severely limited by the inability of MOVE to simulate the control rod program actually used for Yankee, hence the inability of CELLMOVE to correctly predict the spatial distribution of power density and fuel burnup throughout core life. However, experimentally-determined results for the variation of nuclide concentrations with burnup could be used in a valid comparison with CELL, and for completeness, with FUEL predictions, without the need to utilize dubious control simulations, i.e., by comparing with the point-depletion results from CELL. Reactivity and discharge burnup predictions for Yankee are compared with experimental results by Beaudreau (5), but no decisions regarding the accuracy of CELLMOVE can be made using the Yankee data because of the above-mentioned power distribution effects.

Comparison of reactivity and burnup between CELLMOVE and Westinghouse calculations are meaningful when based on the San Onofre Reactor, however, since all reactivity changes occurring under full-power operating conditions are compensated for by adjusting the soluble boron concentration in the water; all control rods are removed from the core upon attainment of full-power operation. This control scheme is adequately simulated by MOVE, and the evaluation of CELL capability can be accomplished with less interference from spatial effects. Comparison of CELL predictions of discharged fuel composition with those calculated by Westinghouse can be used as a further check of the code's accuracy in predicting nuclide concentrations during irradiation. The use of Westinghouse calculations as a basis for comparison is justified due to the high degree of sophistication used in design codes and the normalization of cross-section libraries generally carried out by manufacturers to insure close agreement with actual reactor operating characteristics.

B. Experimental Data for Yankee Reactor

Experimentally-determined nuclide concentrations for Yankee (13) apply to the asymptotic region, i.e., the center of a fuel assembly where control rod and water gap effects are minimized, and are therefore not composite average values for the reactor. Consequently, the CELL code was run using only lattice geometry, i.e., the so-called "extra" region (described in Section III) was not employed for these calculations.

A comparison between the Yankee Reactor experimental data and the calculated results of both the FUEL and CELL codes is given in Figures II.1, II.2, and II.3 for the items of principal interest. Calculations were made using, as nearly as possible, the same geometric and nonfuel cross-section data for the two codes. The Wigner-Wilkins spectrum was calculated

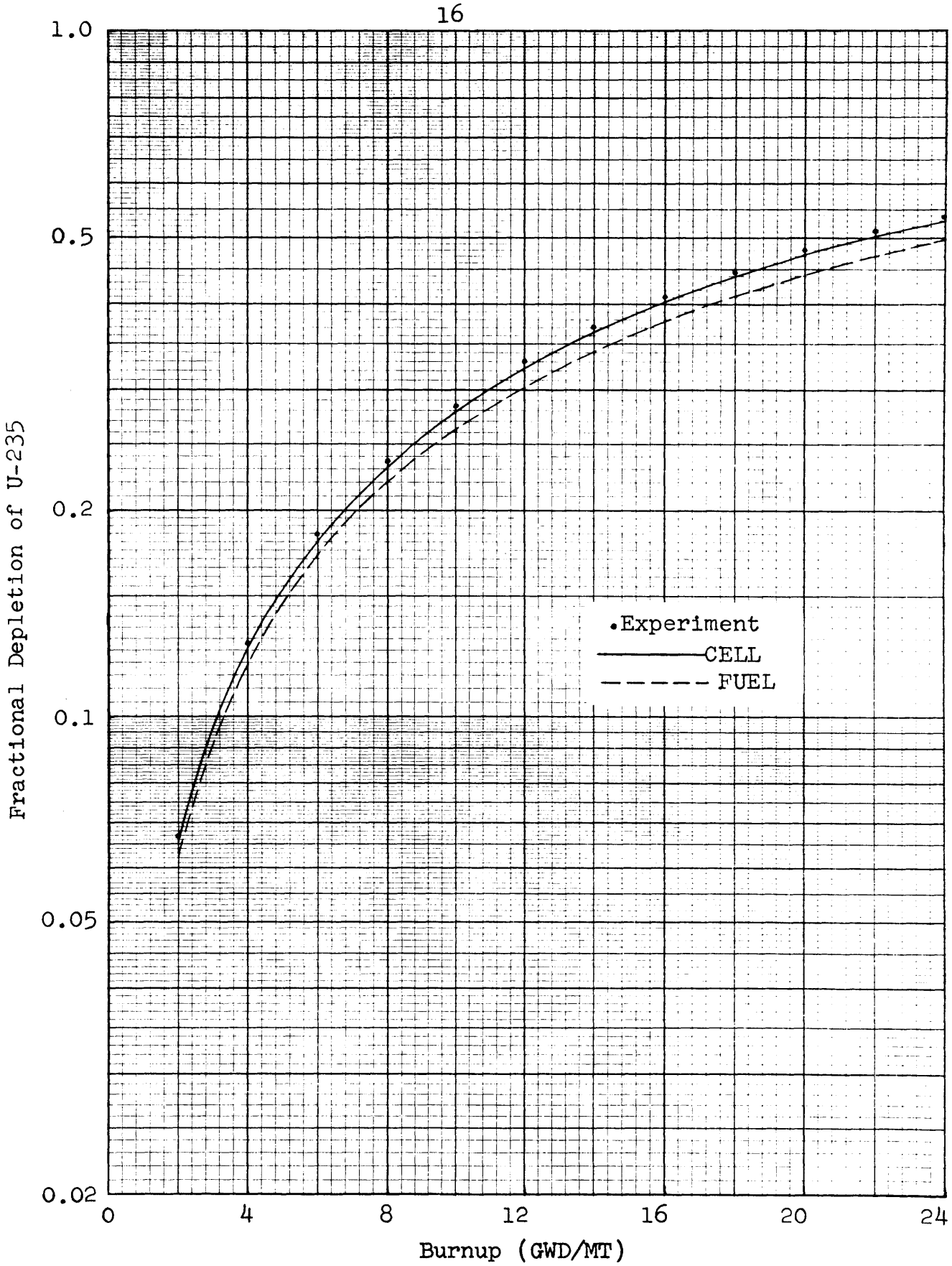

FIGURE II.1 Fractional Depletion of U-235 vs Burnup - Yankee Reactor

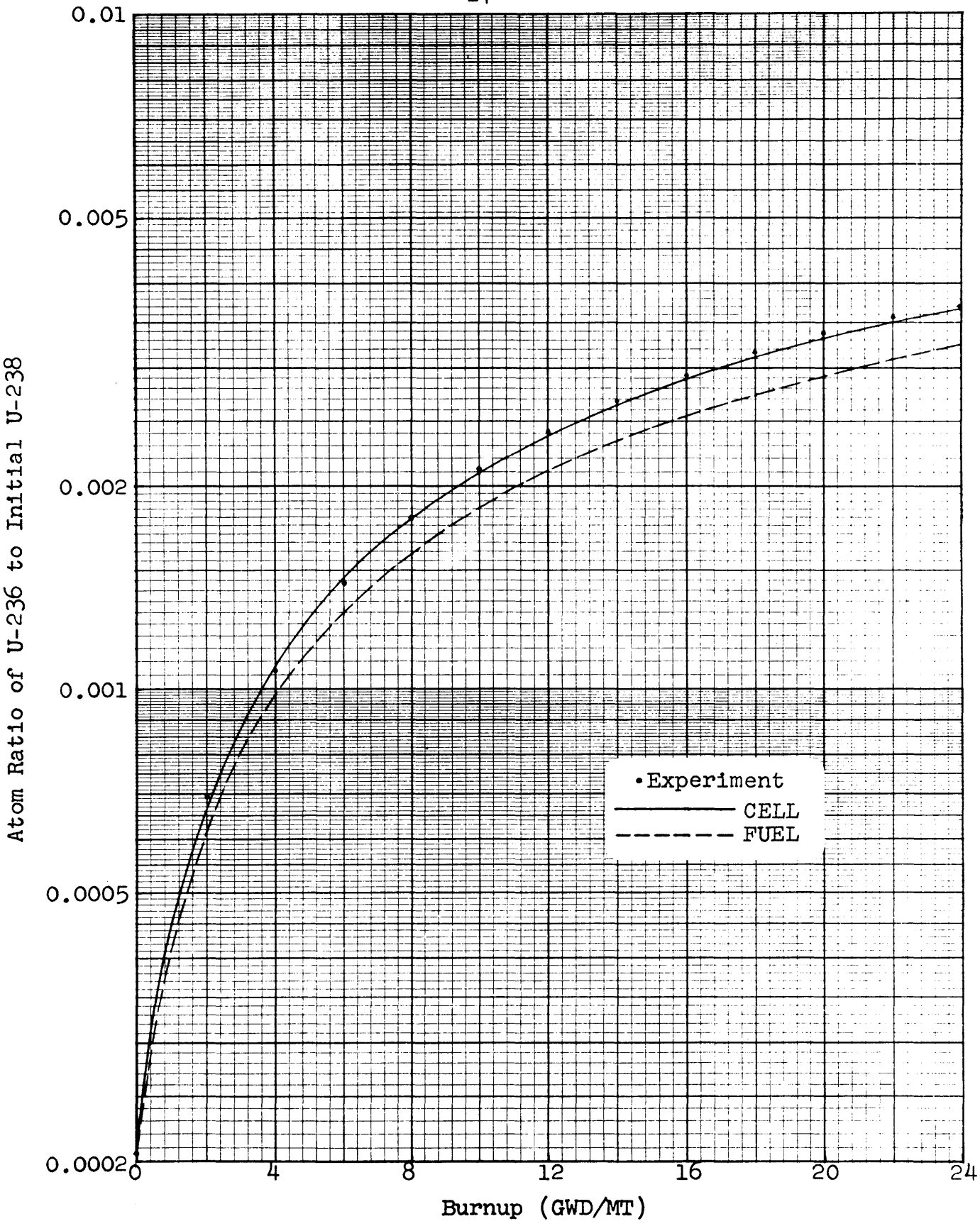

FIGURE II.2 Atom Ratio of U-236 to Initial U-238 vs Burnup - Yankee Reactor

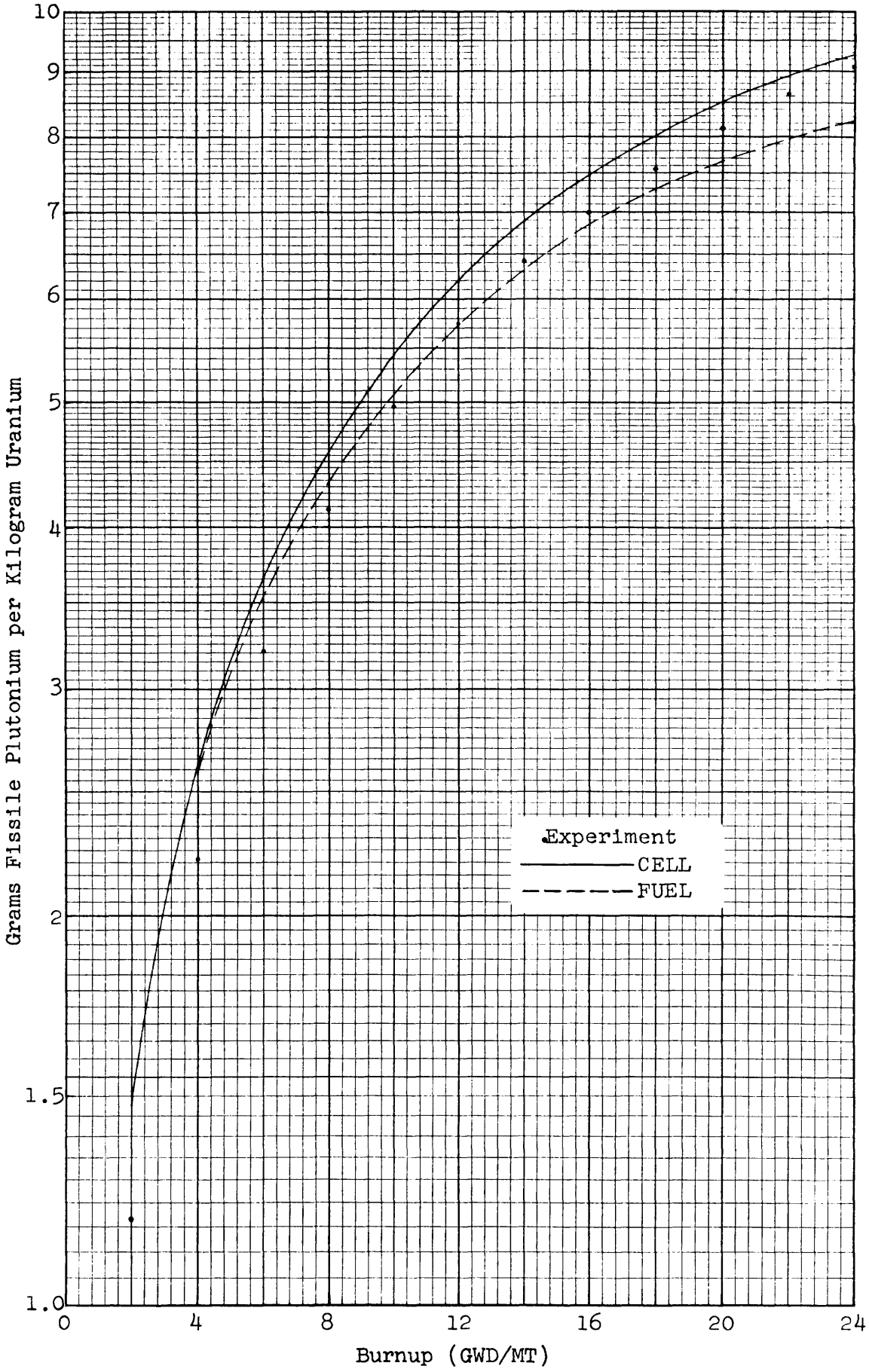

FIGURE II.3 Grams Fissile Plutonium per Kilogram Uranium vs Burnup - Yankee Reactor

by CELL, while FUEL calculations were based, of necessity, on the Wilkins spectrum. The most significant input parameter which is different for the two codes is the thermal cut-off energy. A cut-off energy of 0.414 eV is necessary for FUEL to be consistent with the resonance integral calculation it performs. For CELL, a value of 0.625 eV is used, as this was found to improve results and was believed to be more consistent with the hard spectrum of a light-water reactor.

Predictions of U-235 depletion (Figure II.1) and U-236 concentration (Figure II.2) as functions of burnup are extremely accurate when CELL is used, while FUEL predictions are in considerable error. The accuracy of CELL results was achieved in part by adjusting the fission and absorption resonance integrals of U-235 to values of 180 and 270 barns, respectively, at the beginning of the irradiation. When the unadjusted resonance integrals calculated by CELL -- 226 and 351 barns, respectively -- were used, the errors in predicting U-235 depletion and U-236 concentration became significant, although generally smaller than the errors in the FUEL results.

In predicting the variation of fissile plutonium content with burnup (Figure II.3), neither code gives close agreement with experiment over the entire range of burnup shown; however, as burnup increases toward economically attractive levels (above 20,000 MWD/T), the superiority of CELL becomes clear, although FUEL appears to give results closer to experiment for the lower burnups. Since the overall shape of the build-up curve predicted by CELL is more consistent with the experimental variation than is the shape of the FUEL curve, and since FUEL predictions at high burnup -- where results are of most practical importance -- become very inaccurate, some improvement has been made in predicting fissile plutonium build-up through the use of CELL.

A more detailed discussion of the preceding results as well as a comparison of CELL and FUEL results for other experi-

mentally-determined quantities can be found in Beaudreau's thesis (5).

C. Calculated Results for San Onofre Reactor

The ability of the combined CELLMOVE model to predict the gross characteristics of the San Onofre Reactor was evaluated by using the same U-235 resonance integral adjustments in CELL as were used in the Yankee calculations and by using the uniform poison removal control scheme provided in MOVE.

Calculations were made for the first cycle only, using SS304 cladding and a core with radially-zoned enrichment. The inner region of the core contained uranium enriched to 3.2%, while the middle and outer regions had enrichments of 3.4% and 3.8%, respectively.

Results from CELLMOVE and Westinghouse calculations are given in Table II.1. Several important observations can be made:

1. The reactivity-limited first-cycle average burnup for the core is predicted very accurately by CELLMOVE, as is the U-235 content of the first batch discharged, i.e., the batch located in the innermost part of the core.

2. CELLMOVE predicts the amount of energy released within each region with good accuracy, which indicates that the code is calculating realistic gross power distributions throughout core life and is therefore adequately predicting the incremental burnup incurred by the fuel in each region.

3. Fissile plutonium production is overpredicted by CELLMOVE for this reactor, as it was for Yankee (Figure II.3), and it can be expected that predictions of fissile plutonium content would again improve for higher burnup levels as was noted earlier in the discussion of Yankee results. Since equilibrium burnup levels of 25,000 MWD/T to 35,000 MWD/T are of most practical interest, the error in predicting equilibrium discharged fissile plutonium content is not expected to be large.

TABLE II.1 Predictions of San Onofre Reactor Performance

Conditions	Parameter	Westinghouse Result (12)	CELLMOVE Result
Hot, full power, clean	k_{eff}	1.185	1.243
	ρ (reactivity,%)	15.61	19.53
	ppm Boron	2800	2185
Hot, full power, equilibrium Xe and Sm	k_{eff}	1.152	1.183
	ρ (%)	13.19	15.48
	ppm Boron	2200	1726
	Initial conversion ratio	0.5	0.56
End of life	Cycle burnup (MWD/MT)	13,500	13,494
	Inner region fuel:		
	a/o U-235	1.84	1.84
	kg Pu	126	135
	a/o Pu-240	15	16.3
	a/o Pu-241	9	9.7
	Fractional energy released by region and by material:	In Mid Out	In Mid Out
	U-235	0.28 0.25 0.20	0.266 0.256 0.180
	U-238	0.03 0.03 0.02	0.032 0.030 0.019
	Pu	0.08 0.08 0.03	0.098 0.084 0.035
	Total	0.39 0.36 0.25	0.396 0.370 0.234

4. Beginning-of-life values of k_{eff} calculated by CELLMOVE are considerably higher than the Westinghouse results, while critical boron concentrations are considerably lower. This apparent contradiction is in all liklihood due to the fact that k_{eff} is defined in different ways for the Westinghouse and CELLMOVE models, with the difference in boron concentration (a less arbitrary quantity than k_{eff}) indicating a true underprediction of excess reactivity by CELLMOVE at the beginning of life. It appears that the low initial reactivity predicted by CELLMOVE is largely due to excessive absorption in U-238, a conclusion substantiated by the following observations:

a. The initial conversion ratio predicted by CELLMOVE is too high;

b. CELLMOVE overpredicts both the mass of plutonium at end-of-life and the fractional energy produced from plutonium fissions, indicating that too high a plutonium production rate is being calculated; and

c. CELLMOVE predictions of fissile plutonium content in Yankee fuel (see Figure II.3) were too high, becoming less accurate as burnup decreased toward zero.

Initial reactivity and plutonium buildup predictions by CELLMOVE could undoubtedly be improved by reading in a resonance integral for U-238, rather than using the built-in calculation described in Section III.4, but this was not judged necessary for the present application of the code in Goellner's work (4).

D. Conclusions Regarding Accuracy of CELLMOVE

The CELLMOVE code predicts the burnup dependence of U-235 and U-236 content with a high degree of accuracy, and it can be expected that Np-237 concentrations are also calculated with acceptable accuracy, although the lack of reliable data on Np-237 buildup data for Yankee and San Onofre make it impossible to assess this capability directly. The accuracy of fissile

plutonium predictions is reasonably good at burnup levels of practical interest and estimated reactivity-limited core lifetime is well within the $\pm$ 10% tolerance originally set as a goal for code performance.

The major deficiencies of the code are in predicting reactivity and plutonium concentration early in core life. Their shortcomings are not significant to the realistic prediction of fuel cycle economics for a particular fuel loading scheme.

In summary, CELLMOVE is an adequate code for accurately predicting the fuel cycle characteristics of most importance in estimating fuel cycle costs of PWR systems.

III. CELL CODE DESCRIPTION

A. General

The CELL code is a modified-two-group point-depletion code written to prepare data for use by the fuel management code, MOVE. The code is written in FORTRAN II source language.

CELL assumes that the irradiation history of fuel containing uranium and/or plutonium can be adequately represented as a function of a single variable -- thermal flux-time -- and that the unit reactor cell can be represented by a volume- and flux-weighted homogenized unit cell. Nuclide concentrations and other properties of the unit cell are transferred as functions of flux-time to either punched cards or to binary tape for subsequent use by MOVE.

Eight nuclides are considered in the calculation, the overall chain beginning with U-235 and terminating with Pu-242, while two groups of equilibrium fission products, a separate accounting of the nonsaturating fission product pairs produced by the four fissioning nuclides (U-235, U-238, Pu-239, and Pu-241), and from two to seven nonfuel materials are accounted for. The general procedure followed within the code is as follows:

1) General input and control data are read in. Principal input data include initial concentrations of all nuclides in the unit cell, volume fractions of five regions, geometric data for the fuel pin and lattice, cross-sections and resonance integrals for the nonfuel regions and miscellaneous operating parameters. In addition, thermal point cross-sections and resonance group data, corresponding to an input thermal cut-off energy, are required. As options, U-238 resonance integral data and/or control poison cross-sections for each flux-time step may be read in. Values for control poison macroscopic absorption cross-sections are used only in the thermal spectrum calculation and do not become part of the data supplied to MOVE. A detailed description of CELL input is given by Beaudreau (5).

2) Quantities which remain constant throughout core life are specified or calculated. These include certain basic nuclear data which have been written into the code.

3) Resonance escape and absorption probabilities are computed using resonance integrals which are calculated for all fuel nuclides and which were read in for fission products and nonfuel materials.

4) Effective thermal cross-sections are calculated for all fuel nuclides, Xe-135, and the nonfuel materials by averaging input thermal cross-sections over a thermal spectrum calculated from either the Wigner-Wilkins or Wilkins models.

5) Using these thermal and resonance parameters, unit cell properties are determined, and new nuclide concentrations are computed at the next flux-time by a fourth-order Runge-Kutta-Gill (21) solution of the nuclide differential equation.

6) Using a constant flux-time interval, Steps 3, 4, and 5 are repeated a specified number of times to obtain the unit cell history over a flux-time range sufficient for the expected residence time of the fuel in the reactor core.

7) Data required by MOVE are punched on cards and/or are written on magnetic tape, in a form suitable for use as MOVE input. Various printout options are available, all under input control.

8) The overall procedure can be repeated for any number of subsequent CELL cases.

The major assumption of CELL is that the nuclide concentrations and unit cell properties are functions of flux-time alone and independent of flux magnitude and flux history. Flux magnitude dependence of a nuclide concentration occurs when the decay rate of the nuclide is of the same order of magnitude as its absorption rate, which is proportional to flux. Xe-135 has this characteristic, as does Pu-241 to a lesser extent. For Xe-135, a flux-time-dependent maximum absorption cross-section is calculated and transferred to MOVE, with the actual

xenon absorption cross-section obtained by MOVE by applying a flux-dependent fraction to the flux-independent maximum absorption cross-section. The effect of Pu-241 decay is of little significance at flux levels encountered in power reactors but is approximated (as seen in Section III.B.6) by computing a decay-to-absorption rate using the volume-averaged thermal flux of the homogenized cell.

A source of dependence on fast flux history is the dependence of resonance reation rates on the fast nonleakage probability. This does not create serious difficulty provided the reactor has a small resonance reaction rate compared with that at thermal energies, or provided an accurate estimate of the fast nonleakage probability is available, remains relatively constant during irradiation, and is approximately the same in all parts of the reactor. Since large thermal power reactors have relatively low fast leakage, tend to have more thermalized spectra than small reactors, and the reflector savings treatment of MOVE becomes less accurate as reactor size decreases, the use of CELLMOVE can be expected to give more accurate results as reactor size increases.

B. Theory

1. Geometric Configuration

The unit cell is comprised of five regions -- fuel meat, fuel pin void, cladding, coolant (or coolant moderator), and "extra". The first four are taken as annular regions in cylindrical geometry, with fuel pins arranged in either a square or hexagonal array.

The concept of an "extra" region was developed by Westinghouse (9) for PWR's to account for the materials that are in the active core region but not in the regular fuel lattice, e.g., control rod followers, water slots, structural support, etc. It is desirable to account for these materials separately since certain parameters such as the fast fission factor, U-238

resonance integral, and thermal disadvantage factors depend almost entirely on the materials and geometry of the regular fuel lattice alone.

To minimize off-computer computation, the extra region is specified as containing up to five materials, each having its own number density, microscopic cross-sections, resonance integral, and material-to-coolant thermal flux ratio. Considerable flexibility is therefore provided in describing the properties of the core, and a wide range of reactor types can be examined by CELL by judicious choice of the extra-region materials.

2. Neutron Cycle

The neutron cycle model used in CELL is shown in Figure III.1. The nomenclature is largely self-explanatory, but is listed in detail in Section IV.

Fission neutrons are produced in thermal and resonance reactions, are multiplied by fast fission in U-238 and are diminished by fast leakage to yield the total number of fast neutrons reaching the upper end of the resonance range. During the slowing-down process, concurrent absorptions occur in U-235, U-238, Pu-239, Pu-241, and fission products, with neutron production occurring in the U-235, Pu-239, and Pu-241 resonances. Following this, successive resonance absorptions occur in U-236 and Pu-242, after which concurrent absorptions occur in Pu-240 and Np-237. Finally, resonance absorptions in the nonfuel materials are assumed to occur in the portion of the resonance range below the lowest fuel resonance energies. Although resonance absorptions actually occur throughout the resonance region for all fuel nuclides, the above ordering of absorptions accounts for the fact that the various nuclides have their strongest absorption at different energy levels.

Following the resonance group, the remaining neutrons enter the thermal group, where they are either absorbed or

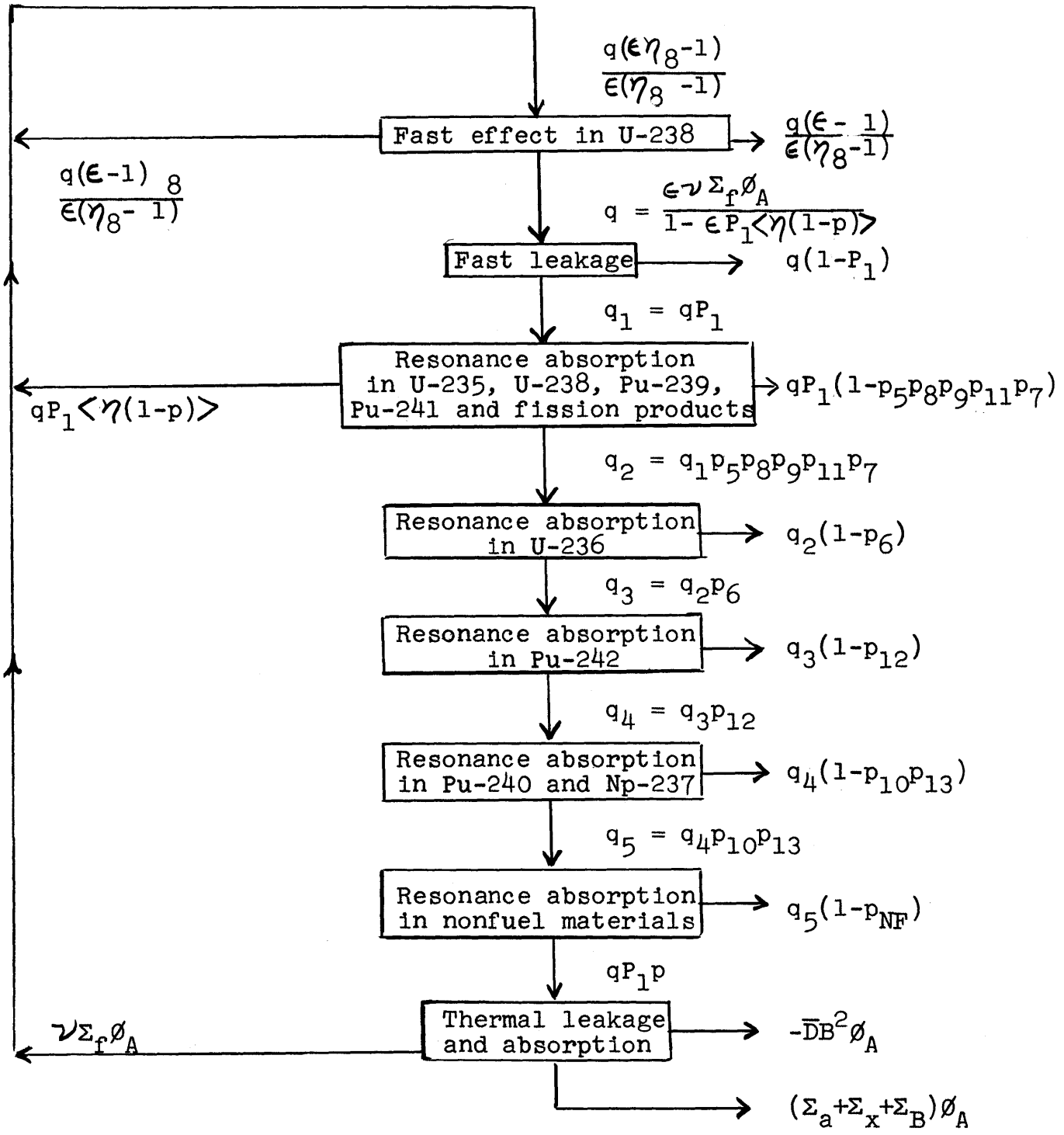

Figure III.1 Neutron Cycle Model for CELL

are lost by leakage from the reactor.

The nuclide notation and subscripting appearing in Figure III.1 is that used throughout this work. In it, 5, 6, and 8 represent U-235, U-236, and U-238, respectively; 7 refers to lumped fission products, which excludes all fission products with thermal cross-sections greater than 10,000 barns; 9, 10, 11, and 12 refer to Pu-239, Pu-240, Pu-241, and Pu-242, respectively; and 13 is Np-237.

3. Treatment of Thermal Group

3.a Microscopic Cross-Sections and Disadvantage Factors

The thermal group extends from zero energy to an input thermal cut-off energy, E_C. The numerical techniques used in the code require that the thermal group be broken up into a specified number of equal neutron velocity intervals, and require that microscopic absorption cross-sections be read in for each velocity point for all fuel nuclides and Xe-135. The absorption cross-sections for all nonfuel materials are assumed to vary according to the 1/v law, so that only 2200 m/sec cross-sections are required. Treatment of fission-product cross-sections is discussed in Section III.B.3.c below. Transport-corrected scattering cross-sections are assumed to be energy-independent throughout the thermal range for all core materials.

Thermal flux disadvantage factors are considered as flux-time- and energy-dependent in the calculation of the thermal flux spectrum and in the subsequent calculation of spectrum-averaged absorption cross-sections. The spectrum is determined at each thermal velocity point, with the velocity x at a general point normalized as

$$x = \sqrt{\frac{E}{k\ T_{mod}}} \qquad (1)$$

with E the neutron energy in eV and T_{mod} the average moderator

temperature in ^{o}K.

The technique employed in calculating disadvantage factors was taken from work done by Strawbridge and Barry (14), who based their work on the integral transport method developed by Amouyal, Benoist, and Horowitz (15). This method enables the calculation of disadvantage factors for cladding, coolant, and fuel-cladding void, based on the average fuel flux. These disadvantage factors are represented by

$$\frac{Y_{CL}(x)}{Y_F(x)} \quad , \quad \frac{Y_C(x)}{Y_F(x)} \quad , \text{ and } \quad \frac{Y_{FS}(x)}{Y_F(x)} \quad ,$$

respectively. $Y_i(x)$ is the flux per unit velocity at normalized velocity x for the region denoted by i, where subscripts CL, F, C, and FS denote the cladding, fuel, coolant, and fuel (meat) surface, respectively. Note that the void region is assigned the same flux magnitude as the fuel surface.

The extra region is treated differently. The energy dependence of the disadvantage factor is assumed to be the same as for the coolant, while the difference between the flux level in each material in the extra region and the flux level in the coolant is accounted for by applying an input energy-independent factor to the coolant disadvantage factor pertinent to that extra region material. In cases where the extra region is a small part of the overall unit cell, e.g., about 10% in a typical PWR, the extra and coolant regions can be assigned the same disadvantage factors with little error.

In CELL, the volume-averaged flux in the overall cell is used as the basis for disadvantage factors, rather than the volume-averaged flux in the fuel used in FUEL. This necessitates the following renormalization of the previously calculated disadvantage factors:

$$\frac{Y_F(x)}{Y(x)} = \frac{1}{A(x)} \qquad (2)$$

$$\frac{Y_{CL}(x)}{Y(x)} = \frac{1}{A(x)} \quad \frac{Y_{CL}(x)}{Y_F(x)} \tag{3}$$

$$\frac{Y_C(x)}{Y(x)} = \frac{1}{A(x)} \quad \frac{Y_C(x)}{Y_F(x)} \tag{4}$$

$$\frac{Y_{FS}(x)}{Y(x)} = \frac{1}{A(x)} \quad \frac{Y_{FS}(x)}{Y_F(x)} \tag{5}$$

$$\frac{Y_E(x)}{Y(x)} = \frac{\phi_E}{\phi_C} \quad \frac{Y_C(x)}{Y(x)} \quad , \tag{6}$$

where $Y(x)$ and $Y_E(x)$ are the volume-averaged flux per unit velocity in the cell and extra region, respectively. The ratio of average flux in the extra region to average flux in the coolant, ϕ_E/ϕ_C, is calculated from

$$\frac{\phi_E}{\phi_C} = \sum_{\ell=1} \left(\frac{\phi_E}{\phi_C}\right)_\ell V_{E,\ell} \quad , \tag{7}$$

where $\left(\frac{\phi_E}{\phi_C}\right)_\ell$ is the specified ratio of the flux in extra region material ℓ to the flux in the coolant, and where $V_{E,\ell}$ is the fraction of total extra region volume occupied by material ℓ. Up to five extra region materials are permitted. The renormalization factor $A(x)$ is determined from

$$A(x) = V_F + V_V \frac{Y_{FS}(x)}{Y_F(x)} + V_{CL} \frac{Y_{CL}(x)}{Y_F(x)} + \left[V_C + V_E \frac{\phi_E}{\phi_C}\right] \frac{Y_C(x)}{Y_F(x)} \quad , \tag{8}$$

where V_F, V_V, V_{CL}, V_C, and V_E are volume fractions for fuel, fuel pin void, cladding, coolant, and extra region, respectively.

3.b Thermal Spectrum

The option exists of calculating the thermal spectrum in

the cell, Y(x), by either the Wilkins (6) or Wigner-Wilkins (7) models. The Wilkins spectrum is calculated using the procedures given by Shanstrom (1), while the Wigner-Wilkins spectrum is determined according to the method utilized in the SOFOCATE code (8). The spectrum-hardening parameter W(x) used in both calculations is calculated as follows for normalized velocity x:

$$W(x) = \frac{\Sigma_{a,T}(x) + D(x)\ B^2}{\xi\ \Sigma_S} \qquad (9)$$

where $\Sigma_{a,T}(x)$ is the homogenized macroscopic absorption cross-section of the cell at velocity x, D(x) is the thermal diffusion coefficient of the cell at velocity x, B^2 is the geometric buckling, and $\xi\ \Sigma_S$ is the slowing-down power of the cell. These are calculated as described below.

$$\Sigma_{a,T}(x) = V_F\ \Sigma_{a,F}(x)\ \frac{Y_F(x)}{Y(x)} + V_{CL}\ \Sigma_{a,CL}\ \frac{Y_{CL}(x)}{Y(x)}$$

$$+ \left[V_C\ \Sigma_{a,C}(x) + V_E\ \Sigma_{a,E}(x) \right]\ \frac{Y_C(x)}{Y(x)} + \Sigma_B(x) \qquad (10)$$

$\Sigma_B(x)$ is the homogenized control poison absorption cross-section at velocity x, which is used in CELL only in estimating the effect of control poison on thermal spectrum hardening. An estimate of the 2200 n/sec control poison macroscopic cross-section can be read in for each flux-time point examined and is assumed to vary as 1/x in determining $\Sigma_B(x)$. The other terms in Equation (10) are self-explanatory, with subscript notation as described earlier. The macroscopic absorption cross-section of the extra region is

$$\Sigma_{a,E}(x) = \sum_{\ell=1}^{5} \left| \frac{\phi_E}{\phi_C} \right|_\ell\ \Sigma_{a,\ell}(x)\ V_{E,\ell} \quad . \qquad (11)$$

If the homogenized transported-corrected scattering cross-

section for the cell is given by $\Sigma_{TR}(x)$, then

$$D(x) = \frac{1}{3\,\Sigma(x)\left[1 - 0.4\,\frac{\Sigma_{a,T}(x)}{\Sigma(x)}\right]^2} \tag{12}$$

where

$$\Sigma(x) = \Sigma_{a,T}(x) + \Sigma_{TR}(x), \tag{13}$$

$$\Sigma_{TR}(x) = V_F\Sigma_{TR,F}\,\frac{Y_F(x)}{Y(x)} + V_{CL}\,\Sigma_{TR,CL}\,\frac{Y_{CL}(x)}{Y(x)} + \left[V_C\,\Sigma_{TR,C} + V_E\,\Sigma_{TR,E}\right]\,\frac{Y_C(x)}{Y(x)}\,, \tag{14}$$

and

$$\Sigma_{TR,E} = \sum_{\ell=1}^{5}\left(\frac{\phi_E}{\phi_C}\right)\,\Sigma_{TR,\ell}\,V_{E,\ell}\,. \tag{15}$$

Finally, using the assumption of a uniform epithermal flux throughout the cell,

$$\xi\,\Sigma_S = V_F(\xi\Sigma_S)_F + V_{CL}(\xi\Sigma_S)_{CL} + V_C(\xi\Sigma_S)_C + V_E(\xi\Sigma_S)_E, \tag{16}$$

where

$$(\xi\,\Sigma_S)_E = \sum_{\ell=1}^{5}(\xi\Sigma_S)\,V_{E,\ell}\,. \tag{17}$$

After calculating Y(x) by either the Wilkins or Wigner-Wilkins procedures, the volume-averaged flux per unit velocity at normalized velocity x can be determined for the fuel, cladding, and coolant regions as follows:

$$Y_F(x) = \left[\frac{Y_F(x)}{Y(x)}\right]\,Y(x) \tag{18}$$

$$Y_{CL}(x) = \left[\frac{Y_{CL}(x)}{Y(x)}\right]\,Y(x) \tag{19}$$

$$Y_C(x) = \left[\frac{Y_C(x)}{Y(x)}\right] Y(x) \qquad (20)$$

The energy dependence of the thermal flux is then known for all regions in the unit cell.

3.c Effective Thermal Cross-Sections

Effective, spectrum-averaged cross-sections are determined for all materials in the unit cell by weighting cross-sections by the appropriate spectrum, integrating over all thermal velocities, and dividing the result by the integral of the cell spectrum Y(x). The divisor is the same in all cases and is given by

$$\phi = \int_0^{x_C} Y(x)\, dx \quad , \qquad (21)$$

where x_C corresponds to the thermal cutoff energy.

For fuel nuclides, the effective microscopic absorption cross-sections are determined from

$$\bar{\sigma}_{a,m} = \frac{\int_0^{x_C} \sigma_{a,m}(x)\, Y_F(x)\, dx}{\phi} \quad , \qquad (22)$$

where $\sigma_{a,m}(x)$ is the absorption cross-section of nuclide m at velocity x and $\bar{\sigma}_{a,m}$ is the effective thermal absorption cross-section for nuclide m. Effective fission cross-sections are found by replacing $\sigma_{a,m}(x)$ by $\sigma_{f,m}(x)$ and $\bar{\sigma}_{a,m}$ by $\bar{\sigma}_{f,m}$ in Equation (22). The effective cross-section for Xe-135, $\bar{\sigma}_x$, is also found by using an equation of this form.

Effective macroscopic absorption cross-sections for the cladding and coolant regions are found from Equations (23) and (24), respectively.

$$\overline{\Sigma}_{a,CL} = \frac{\int_0^{x_C} \Sigma_{a,CL}(x)\ Y_{CL}(x)\ dx}{\phi} \tag{23}$$

$$\overline{\Sigma}_{a,C} = \frac{\int_0^{x_C} \Sigma_{a,C}(x)\ Y_{C}(x)\ dx}{\phi} \quad . \tag{24}$$

Since the coolant and extra region absorption cross-sections are both assumed to vary as 1/x and since both regions are assigned the same thermal-spectrum energy variation, then the effective cross-section for the extra region, $\overline{\Sigma}_{a,E}$, can be written as

$$\overline{\Sigma}_{a,E} = \Sigma_{0,E} \frac{\overline{\Sigma}_{a,C}}{\Sigma_{0,C}} \quad , \tag{25}$$

where $\Sigma_{0,C}$ and $\Sigma_{0,E}$ are the 2200 m/sec macroscopic absorption cross-sections for the coolant and extra regions, respectively, with $\Sigma_{0,E}$ determined as follows:

$$\Sigma_{0,E} = \sum_{\ell=1}^{5} \left(\frac{\phi_E}{\phi_C}\right)_\ell \Sigma_{0,\ell}\ V_{E,\ell} \tag{26}$$

with the 2200 m/sec macroscopic cross-section of extra region material ℓ given by $\Sigma_{0,\ell}$.

The effective thermal diffusion coefficient, $\overline{D}$, is calculated from the following equation:

$$\overline{D} = \frac{\int_0^{x_C} D(s)\ Y(x)\ dx}{\phi} \quad . \tag{27}$$

Fission products are divided into three groups. Xe-135 forms a group by itself, while the remaining fission products with thermal cross-sections greater than 10,000 barns are in a group called the "Samarium group". Both groups reach

equilibrium concentrations very soon after attainment of full-power operation. The third group contains all fission products whose cross-sections are less than 10,000 barns. This group does not reach equilibrium, but accumulates throughout irradiation.

The equilibrium effective cross-section for Xe-135, neglecting loss of Xe-135 by decay, is found as follows:

$$\bar{\Sigma}_{x,M} = \sum_{m=5,9,11} y_{x,m} N_m \sigma_{f,m} + \frac{qP_1}{\phi_A V_F}\left[\frac{y_{x,8}(\epsilon - 1)}{\epsilon P_1 (1+\alpha_8)(\eta_8 - 1)} + \sum_{m=5,9,11} \frac{y_{x,m} \langle 1-p_m \rangle}{1+\alpha_m} \right] , \quad (28)$$

where:

$y_{x,m}$ = Xe-135 fission yield for nuclide m;

N_m = atomic density of fuel nuclide m;

q = slowing-down density of the cell before fast leakage occurs (see Equation (30));

P_1 = fast nonleakage probability;

ϕ_A = absolute magnitude of the volume-averaged thermal flux in the cell (see Equation (31));

ϵ = fast fission factor;

α_m = resonance capture-to-fission ratio of nuclide m;

α_8 = number of fast neutrons produced per fast absorption in U-238; and

$\langle 1-p_m \rangle$ = resonance absorption probability of nuclide m the calculation of which is discussed in Section III.B.4c.

η_8 = number of fast neutrons produced per fast absorption in U-238; and

The actual equilibrium effective Xe-135 cross-section, taking into account Xe-135 decay, is

$$\bar{\Sigma}_x = \bar{\Sigma}_{x,m} \frac{\phi_A}{\phi_A + \lambda_x/\bar{\sigma}_x} \quad , \tag{29}$$

where λ_x is the decay constant for Xe-135.

The equilibrium effective cross-section for the Samarium group, $\bar{\Sigma}_{Sm}$, is calculated using an equation identical to Equation (28) for $\bar{\Sigma}_{x,m}$, except that the fission yield for the Samarium group, $y_{S,m}$, replaces the fission yield for Xe-135, $y_{x,m}$, in all places.

The factor qP_1/ϕ_A appears not only in the equations for $\bar{\Sigma}_{x,M}$ and $\bar{\Sigma}_{Sm}$ but also in other equations presented later. This is the slowing-down density entering the resonance range per unit of average thermal flux in the cell, and is calculated from

$$\frac{qP_1}{\phi_A} = \frac{(\nu \Sigma_f)}{\frac{1}{\epsilon P_1} - \langle \eta(1-p) \rangle} \quad , \tag{30}$$

where $(\upsilon \Sigma_f)$ and $\langle \eta(1-p) \rangle$ are the number of neutrons released by thermal fissions per unit of thermal flux and by resonance fissions per unit of slowing-down density entering the resonance range, respectively, as calculated by Equations (73) and (75).

The calculation of ϕ_A is performed as follows:

$$\phi_A = \frac{\overline{P}}{1.602 \times 10^{-12} \sum_{m=5,8,9,11} E_m} , \tag{31}$$

where $\overline{P}$ is the average power density in the cell in kw/l and E_m is given by

$$E_m = R_m \left(V_f N_m \sigma_{f,m} + \frac{qP_1}{\phi_A} \frac{\langle 1 - p_m \rangle}{1 + \alpha_m} \right) \tag{32}$$

for m = 5,9,11 and by

$$E_8 = R_8 \frac{qP_1}{\phi_A} \left[\frac{\epsilon - 1}{\epsilon P_1 (1+\alpha_8)(\eta_8 - 1)} \right] \tag{33}$$

for U-238. In Equations (32) and (33), R_m is the energy released per fission in nuclide m, in MeV.

The third group of fission products has an effective macroscopic absorption cross-section $\overline{\Sigma}_{FP}$, equal to

$$\overline{\Sigma}_{FP} = N_7 \overline{\sigma}_{a,7}, \tag{34}$$

where N_7 is the number of "lumped" fission product pairs present and $\overline{\sigma}_{a,7}$ is the effective absorption cross-section per pair. If $\sigma_{a,7}(x)$ is assumed to vary as 1/x and if $\sigma_{a,8}(x)$ is likewise assumed to vary as 1/x below the thermal cutoff energy, then

$$\overline{\sigma}_{a,7} = \frac{\overline{\sigma}_{a,8}}{\sigma_{0,8}} \hat{\sigma}_7 , \tag{35}$$

where $\overline{\sigma}_{a,8}$ has been calculated previously (see Equation (22)),

$\sigma_{0,8}$ is the 2200 m/sec absorption cross-section for U-238, and $\hat{\sigma}_7$ is the 2200 m/sec absorption cross-section per pair for the "lumped" third group of fission products. CELL uses the method developed by Hurst (16) for determining $\hat{\sigma}_7$ as a function of flux-time, thereby accounting for the change of the absorption characteristics of lumped fission products as irradiation proceeds.

4. Treatment of Resonance Group

4.a General Procedure

To obtain resonace reaction rates, the resonance escape and absorption probabilities of the fuel nuclides must be computed. Absorption probabilities are then multiplied by qP_1/ϕ_A to form resonance reaction rates per unit of thermal flux. Neutron production in the resonance group is calculated for three nuclides - U-235, Pu-239, and Pu-241 - and it is assumed that these nuclides have the same neutron production per fission, ν_m, in the resonance region as in the thermal region; however, the capture-to-fission ratios in the resonance region, α_m, are recalculated from effective fission and absorption resonance integrals at each flux-time step.

Resonance absorption for the Samarium fission product group is implicity included by defining the equilibrium cross-section, $\bar{\Sigma}_{Sm}$, as that required to balance total (from all sources) Samarium group production and destruction. The same reasoning applies to the Xe-135 cross-section when Xe-135 decay is neglected (Equation (28)); however, the ratio of $\bar{\Sigma}_x$ to $\bar{\Sigma}_{x,m}$ considers only thermal absorption in Xe-135 (see Equation (29)). Neglect of resonance absorption in Xe-135 in this respect is not significant because of the predominance of the thermal cross-section.

The resonance integrals for all fuel nuclides except U-238 are computed by a numerical integration over the resonance energy range, which is divided into a specified (up to 300)

number of lethargy intervals. This calculation requires that the lethargy width and corresponding cross-sections for all fuel nuclides be provided (as input) for each interval.

4.b Effective Resonance Integrals

The basic assumption in calculating resonance integrals for all fuel nuclides is that the "Narrow Resonance, Infinite Mass Approximation" (NRIA) (17) is valid for all fuel nuclide resonances. To attempt to use more than one approximation would be both numerically cumbersome and unrewarding in comparison with the additional computer time required, since most resonances, particularly those which contribute most to the total resonance integrals, have characteristics which make the NRIA approximation valid.

The equation used to calculate the effective absorption resonance integral I_m of nuclide m is as follows for all nuclides except U-238 and the lumped fission product group:

$$I_m = \int_{E_C}^{\bar{E}_F} \frac{\Sigma_{PC} + \frac{\gamma S}{4V}}{\Sigma_{PC} + \frac{\gamma S}{4V} + \Sigma_a^{res}(E)} \sigma_{a,m}^{res}(E) \frac{dE}{E} , \qquad (36)$$

where $\bar{E}_F$ is the mean energy of the fission spectrum;

Σ_{PC} is the potential scattering cross-section of the low-atomic-weight atoms associated with the fuel, e.g., oxygen atoms in UO_2;

S is the fuel (meat) surface area per unit length of fuel pin;

V is the fuel volume per unit length of fuel pin;

$\sigma_{a,m}^{res}(E)$ is the resonance absorption cross-section for nuclide m at energy E;

$\Sigma_a^{res}(E)$ is the macroscopic absorption cross-section of the fuel nuclides at energy E, calculated from

$$\Sigma_a^{res}(E) = \sum_m N_m \sigma_{a,m}^{res}(E) \quad , \tag{37}$$

with m = 5 to 13, excluding m = 7; and

γ is the effective shielding factor for the lattice, calculated from (14)

$$\gamma = \frac{\psi}{1 + 0.1\,(1 - \psi)} \quad , \tag{38}$$

where ψ is the blackness of the nonfuel portion of the lattice, calculated by the method of Sauer (18) for either square or hexagonal lattice geometries.

The effective fission resonance integral $I_{f,m}$ is calculated for m = 5,9, and 11 by inserting the fission cross-section $\sigma_{f,m}^{res}(E)$ into Equation (36) in place of $\sigma_{a,m}^{res}(E)$, with all other terms, including $\Sigma_a^{res}(E)$, unchanged. The resonace capture-to-fission ratio, α_m, for m = 5,9, and 11 is calculated as follows:

$$\alpha_m = \frac{I_m}{I_{f,m}} - 1 \quad . \tag{39}$$

The resonance integral for U-238, I_8, can either be read in as input - as constant during irradiation or as a function of flux-time - or can be calculated by CELL using a correlation developed by Strawbridge and Barry (14) for uranium metal and oxide fuel. It is probable that the correlation can be applied with success to uranium carbide and uranium alloys as well (14). The correlation, described below, is particularly useful in that it includes dependence of the resonance integral upon the average fuel temperature T_F (^oK), i.e., it accounts for Doppler effects. The calculation of I_8 proceeds as follows:

$$I_8 = \beta\, I_{8,C} \tag{40}$$

where $I_{8,C}$ is the resonance integral calculated from the

correlation, and β is a correction factor defined as the ratio of the U-238 resonance integral calculated using Equation (36) to the U-238 resonance integral calculated by replacing $\Sigma_a^{res}(E)$ with $N_8\sigma_{a,8}^{res}(E)$ in Equation (36). The correlation is

$$I_{8,C} = 2.16\ y + 2.56 + (0.0279\ y - 0.0537)\ T_F^{1/2} , \qquad (41)$$

where the scattering parameter y is given by

$$y = \left[\frac{\Sigma_{PT}}{N_8} (1-P_C) + \frac{\gamma S}{4VN_8} \right]^{1/2} . \qquad (42)$$

Σ_{PT} is the macroscopic potential scattering cross-section of the fuel molecules and P_C is the collision probability for resonance group neutrons in the fuel, as calculated by Sauer's (18) method.

Infinite dilution resonance integrals for lumped fission product pairs from U-235 and from a group comprising U-238, Pu-239, and Pu-241 are supplied as input data. These initial values are assumed to change during irradiation such that the ratio of resonance integral to $\hat{\sigma}_7$ is constant for all points in time. The composite infinite dilution resonance integral, I_7^{∞}, is found by weighting the resonance integrals for U-235 and U-238 + Pu-239 + Pu-241 fission product pairs by the fraction of total accumulated lumped fission product pairs resulting from fissions in each. To obtain the effective resonance integral I_7 for lumped fission product pairs, the following Crowther-Weil (11) - type equation is used:

$$I_7 = \frac{I_7^{\infty}}{1 + \frac{N_7\ I_7^{\infty}}{\Sigma_{PT}}} . \qquad (43)$$

The effective resonance integrals for the cladding (I_{CL}) and coolant (I_C) regions and for the five materials of the

extra region are read in as input data and are all assumed to be constant throughout irradiation, since their concentrations remain virtually unchanged. The resonance integral for the extra region, I_E, is then computed as follows:

$$I_E = \sum_{\ell=1}^{5} N_{E,\ell}\ I_{E,\ell}\ V_{E,\ell} \quad , \tag{44}$$

where $N_{E,\ell}$ and $I_{E,\ell}$ are the number density and resonance integral, respectively, of material ℓ in the extra region.

4.c Resonance Escape and Absorption Probabilities

Resonance escape probabilities are calculated for fuel (p_F), cladding (p_{CL}), coolant (p_C), and for the extra region (p_E). For the fuel region, escape probabilities are calculated for all fuel nuclides and for the lumped fission product pairs.

The escape probability for nuclide m is calculated from

$$p_m = \exp\left(-\frac{V_F\ N_m}{\xi\ \Sigma_S} I_m\right) \tag{45}$$

for m = 5 to m = 13, while the overall escape probability for the fuel region, p_F, is

$$p_F = \prod_{m=5}^{13} p_m \quad . \tag{46}$$

For the three nonfuel regions, the following equation is used for the escape probability

$$p_i = \exp\left(-\frac{V_i\ N_i}{\xi\ N_S} I_i\right) \quad , \tag{47}$$

where i = CL for the cladding, i = C for the coolant, and i = E for the extra region.

The overall resonance escape probability for the unit

cell is then calculated from

$$p = p_F p_{CL} p_C p_E \quad . \tag{48}$$

The resonance absorption probability is needed for each of the fuel nuclides and for the lumped fission products in order to compute the buildup and depletion of these nuclides as well as to determine the number of neutrons released in resonance group fissions.

For calculating resonance absorption rates in the fuel nuclides, the resonance group is broken up into six subgroups. Fast leakage occurs in the subgroup having highest energy, absorption by the fuel nuclides occurs in the mext four subgroups, and absorption by the nonfuel materials occurs in the subgroup of lowest energy. The slowing-down density is assumed to be depleted by the leakage and absorption processes according to the energy sequence of the subgroups.

The assignment of nuclides to the various fuel absorption subgroups is determined by the general energy range wherein most resonance absorptions occur for each nuclide. Since most nonfuel materials have cross-sections which obey the 1/v law, they are assumed to have most of their absorptions at lower energies than do any of the fuel nuclides. In order of decreasing energy, the makeup of each subgroup is as follows:

(1) Fast leakage
(2) Absorptions in U-235, U-238, Pu-239, Pu-241, and lumped fission products
(3) Absorption in U-236
(4) Absorption in Pu-242
(5) Absorptions in Pu-240 and Np-237
(6) Absorptions in nonfuel materials

For absorber m, $\langle 1 - p_m \rangle$ is the probability of an absorption occurring during the slowing-down of a neutron through the resonance energy range. The following equations are used.

For m = 5,7,8,9,11:

$$\langle 1 - p_m \rangle = \frac{N_m I_m}{N_5 I_5 + N_7 I_7 + N_8 I_8 + N_9 I_9 + N_{11} I_{11}} (1 - p_5 p_7 p_8 p_9 p_{11}) \tag{49}$$

For m = 6

$$\langle 1 - p_6 \rangle = p_5 p_7 p_8 p_9 p_{11} (1 - p_6) \tag{50}$$

For m = 12

$$\langle 1 - p_{12} \rangle = p_5 p_7 p_8 p_9 p_{11} p_6 (1 - p_{12}) \tag{51}$$

For m = 10, 13:

$$\langle 1 - p_m \rangle = p_5 p_7 p_8 p_9 p_{11} p_6 p_{12} \left(\frac{N_m I_m}{N_{10} I_{10} + N_{13} I_{13}}\right)(1 - p_{10} p_{13}) \tag{52}$$

5. Fast Fission Effect

The fast fission effect, ϵ, is defined as the number of neutrons slowing down past the fission threshold of U-238 per fast neutron produced by thermal and resonance fissions. The equation used for ϵ is given symbolically as

$$\epsilon = 1 + \left[\frac{\nu_8 - (1 + \alpha_8)}{\nu_5}\right] \delta_8 \quad , \tag{53}$$

where ν_5 and ν_8 are the number of neutrons released per fission in U-235 and U-238, respectively, and δ_8 is the ratio of total fissions in U-238 to total fissions in U-235. Measurements performed by Klein et al. (19) for water-moderated, slightly-enriched

uranium metal and oxide lattices indicate no significant dependence of δ_8 on rod size, the chemical form of uranium, or uranium enrichment. An analytical expression for the dependence of these measured results on hydrogen-to-uranium atom ratio was prepared by Wehmeyer (20). Using Wehmeyer's expression for δ_8 with values for ν_5, ν_8, and α_8 of 2.43, 2.79, and 0.1907, respectively, the equation for becomes

$$\epsilon = 1.0036 + 0.1224 \left(\frac{V_C \, N_H}{V_F \, N_U}\right)^{-0.764} , \qquad (54)$$

where N_H is the number density of hydrogen in the coolant and N_U is the number density of uranium in the fuel.

CELL will either calculate ϵ at initial full-power conditions using Equation (54) or will accept an input value for . In either case, ϵ is assumed to remain constant throughout the cycle.

6. Nuclide Concentration Equations

Number densities of all fuel nuclides and the three fission product groups are recalculated at each flux-time step. For the Xe-135 and Samarium groups of fission products, the effective macroscopic absorption cross-sections, rather than number densities, are calculated according to the procedures outlined previously in Section III.B.3c. The overall density of lumped fission product pairs is calculated as the sum of the separate densities of lumped fission product pairs from fissions in U-235, U-238, Pu-239, and Pu-241. This is done to permit a calculation of fuel exposure which accounts for differences in R_m, the energy released per fission in nuclide m (in MeV).

The time-derivative of the U-235 number density can be written as

$$\frac{dN_{25}}{dt} = - N_5 \overline{\sigma}_{a,5} \phi_A - \frac{qP_1}{V_F} \langle 1 - p_5 \rangle . \qquad (55)$$

After dividing both sides of Equation (55) by ϕ_A, the equation can be rewritten as

$$\frac{dN_{25}}{d\theta} = - N_{25} \overline{\sigma}_{a,5} - \frac{qP_1}{\phi_A V_F} \langle 1 - p_5 \rangle , \qquad (56)$$

where θ, the thermal flux-time, is given by

$$\theta = \int_0^t \phi_A(t)\, dt \quad , \qquad (57)$$

so that the differential $d\theta$ is just $\phi_A dt$. Equation (56) is in the form desired for solution by CELL. Similarly, equations for the other nuclides can be obtained. These are listed below, with the U-235 equation repeated for completeness:

U-235:
$$\frac{dN_5}{d\theta} = - N_5 \overline{\sigma}_{a,5} - \frac{qP_1}{\phi_A V_F} \langle 1 - p_5 \rangle \qquad (56)$$

U-236:
$$\frac{dN_6}{d\theta} = N_5(\overline{\sigma}_{a,5} - \overline{\sigma}_{f,5}) - N_6 \overline{\sigma}_{a,6} + \frac{qP_1}{\phi_A V_F} \left[\frac{\alpha_5 \langle 1 - p_5 \rangle}{1 + \alpha_5} - \langle 1 - p_6 \rangle \right] \qquad (58)$$

U-238:
$$\frac{dN_8}{d\theta} = - N_8 \overline{\sigma}_{a,8} - \frac{qP_1}{\phi_A V_F} \left[\langle 1 - p_8 \rangle + \frac{\epsilon - 1}{\epsilon P_1 (\eta_8 - 1)} \right] \qquad (59)$$

Pu-239:
$$\frac{dN_9}{d\theta} = N_8 \overline{\sigma}_{a,8} - N_9 \overline{\sigma}_{a,9} + \frac{qP_1}{\phi_A V_F} \left[\langle 1 - p_8 \rangle - \langle 1 - p_9 \rangle + \frac{\alpha_8 (\epsilon - 1)}{\epsilon P_1 (\eta_8 - 1)(1 + \alpha_8)} \right] \qquad (60)$$

Pu-240: $$\frac{dN_{10}}{d\theta} = N_9(\bar{\sigma}_{a,9} - \bar{\sigma}_{f,9}) - N_{10}\bar{\sigma}_{a,10} + \frac{qP_1}{\phi_A V_F}\left[\frac{\alpha_9 \langle 1 - p_9\rangle}{1 + \alpha_9} - \langle 1 - p_{10}\rangle\right] \quad (61)$$

Pu-241: $$\frac{dN_{11}}{d\theta} = N_{10}\bar{\sigma}_{a,10} - N_{11}(\bar{\sigma}_{a,11} + \frac{\lambda_{11}}{\phi_A}) + \frac{qP_1}{\phi_A V_F}\left[\langle 1 - p_{10}\rangle - \langle 1 - p_{11}\rangle\right] \quad (62)$$

Pu-242: $$\frac{dN_{12}}{d\theta} = N_{11}(\bar{\sigma}_{a,11} - \bar{\sigma}_{f,11}) - N_{12}\bar{\sigma}_{a,12} + \frac{qP_1}{\phi_A V_F}\left[\frac{\alpha_{11}\langle 1 - p_{11}\rangle}{1 + \alpha_{11}} - \langle 1 - p_{12}\rangle\right] \quad (63)$$

Np-237: $$\frac{dN_{13}}{d\theta} = N_6\bar{\sigma}_{a,6} - N_{13}\bar{\sigma}_{a,13} + \frac{qP_1}{\phi_A V_F}\left[\langle 1 - p_6\rangle - \langle 1 - p_{13}\rangle\right] \quad (64)$$

Note that the decay of U-237 to Np-237 and the successive decays from U-239 to Np-239 to Pu-239 have been assumed to occur instanteously for the purposes of this calculation. Note also that nuclide 13 is Np-237 in CELL, while in FUEL (2) nuclide 13 represents an optional burnable poison which is not permitted in CELL.

Nuclide numbers 14 through 17 are assigned to the lumped fission product pairs arising from fissions in the following nuclides:

U-238 fissions: $$\frac{dN_{14}}{d\theta} = \frac{q}{\phi_A V_F}\left[\frac{\epsilon - 1}{\epsilon(\eta_8 - 1)(1+\alpha_8)}\right] \quad (65)$$

U-235 fissions: $$\frac{dN_{15}}{d\theta} = N_5\overline{\sigma}_{f,5} + \frac{qP_1}{\phi_A V_F}\left[\frac{\langle 1 - p_5\rangle}{1 + \alpha_5}\right] \quad (66)$$

Pu-239 fissions: $$\frac{dN_{16}}{d\theta} = N_9\overline{\sigma}_{f,9} + \frac{qP_1}{\phi_A V_F}\left[\frac{\langle 1 - p_9\rangle}{1 + \alpha_9}\right] \quad (67)$$

Pu-241 fissions: $$\frac{dN_{17}}{d\theta} = N_{11}\overline{\sigma}_{f,11} + \frac{qP_1}{\phi_A V_F}\left[\frac{\langle 1 - p_{11}\rangle}{1 + \alpha_{11}}\right] \quad (68)$$

Thus, the buildup of the composite lumped fission products can be written as

$$\frac{dN_7}{d\theta} = \frac{dN_{14}}{d\theta} + \frac{dN_{15}}{d\theta} + \frac{dN_{16}}{d\theta} + \frac{dN_{17}}{d\theta} \quad . \quad (69)$$

The coupled system of differential equations -- Equations (56) and (58) through (67) -- is solved by a fourth-order Runge-Kutta-Gill procedure described by Romanelli (21). Number density solutions are obtained for a specified number of flux-time interval $\Delta\theta$. Number densities at the n^{th} flux-time point θ_n are obtained from the Runge-Kutta-Gill procedure using the known number densities at the (n-1)st flux-time point as starting values, where

$$\theta_n = \theta_{n-1} + \Delta\theta \ , \quad (70)$$

and assuming that all cross-sections and resonance integrals remain constant over the flux-time step.

At each flux-time point, the fuel exposure B is calculated in MWD/MT according to the following equation:

$$B = \frac{1116765^*}{\sum_{m=5}^{13} M_m N_m^o}\left(R_8N_{14} + R_5N_{15} + R_9N_{16} + R_{11}N_{17}\right) \ , \quad (71)$$

where M_m and N_m^o are the mass per gram-mole and initial number

*$1116765 = \frac{\text{atoms}}{\text{gm atoms}} \times \frac{\text{MWD}}{\text{MeV}} \times \frac{\text{gm}}{\text{T}}$

density of nuclide m, respectively.

7. Properties Calculated for Use by MOVE Code

In addition to various control parameters, flux-time-independent values for ϵ and $\overline{D}$ are transferred to MOVE either by binary tape or by punched cards suitable for use by MOVE. Similarly transferred to MOVE are various flux-time-dependent unit cell properties, values for which are supplied for the time-zero, poisoned (with equilibrium Xe and Sm) condition and for each of a specified number of equally-spaced flux-time points considered by CELL. The properties transferred are listed below.

(a) Number densities, N_m, for nuclides m=5 through m=13;

(b) Homogenized macroscopic thermal fission cross-section,

$$\Sigma_f = V_F \sum_{m=5,9,11} N_m \overline{\sigma}_{f,m} \quad ; \tag{72}$$

(c) Number of neutrons released by thermal fissions per unit of thermal flux,

$$(\nu\Sigma_f) = V_F \sum_{m=5,9,11} \nu_m N_m \overline{\sigma}_{f,m} \quad ; \tag{73}$$

(d) Number of resonance fissions per unit of slowing-down density entering the resonance region,

$$\left\langle \frac{1 - p}{1 + \alpha} \right\rangle = \sum_{m=5,9,11} \frac{\langle 1 - p_m \rangle}{1 + \alpha_m} \quad ; \tag{74}$$

(e) Number of neutrons released by resonance fissions per unit of slowing-down density entering the resonance region,

$$\langle \eta(1 - p) \rangle = \sum_{m=5,9,11} \frac{\nu_m \langle 1 - p_m \rangle}{1 + \alpha_m} \quad ; \tag{75}$$

(f) Overall resonance escape probability, p;

(g) Homogenized macroscopic absorption cross-section for Xe-135, neglecting Xe-135 decay,

$$\Sigma_{x,M} = V_F \bar{\Sigma}_{x,M} \text{ ; and} \tag{76}$$

(h) Homogenized cell macroscopic absorption cross-section excluding Xe-135,

$$\Sigma_a = V_F \left[\sum_{m=5}^{13} N_m \bar{\sigma}_{a,m} + \bar{\Sigma}_{Sm} \right] + V_{CL} \bar{\Sigma}_{a,CL} + V_C \bar{\Sigma}_{a,C} + V_E \bar{\Sigma}_{a,E} \, . \tag{77}$$

8. Definition of k_∞

The infinite medium multiplication factor k_∞ is calculated for both clean and poisoned initial conditions and at all subsequent flux-time points. The equation used is only one of a number which could be used, but the choice of a definition for k_∞ is not a matter of practical importance, since the significant reactivity calculation is performed by MOVE (2). The equation is:

$$k_\infty = \frac{\text{rate of production of thermal neutrons}}{\text{rate of consumption of thermal neutrons}}$$

$$k_\infty = \frac{\epsilon \, p \, (\nu \Sigma_f)}{\left[1 - \epsilon \langle \eta (1-p) \rangle\right] \left[\Sigma_a + V_F \bar{\Sigma}_x \right]} \, . \tag{78}$$

9. Constant Nuclear Data

A large block of constant data -- both operational and nuclear -- is incorporated into CELL for use in all cases. A complete listing of this data is given by Beaudreau (5). The constant nuclear data of principal interest is listed in Table III.1. Definitions of all items have been given in the

text and can also be found in Appendix A, Nomenclature.

C. Flow of Logic

Detailed logical flow diagrams for the CELL main program and subroutines are given by Beaudreau (5). A broad descriptive logical flow diagram of the CELL code as a whole is shown in Figure III.2.

Table III.1 CONSTANT NUCLEAR DATA

Item	Value
$\sigma_{o,8}$	2.71 barns
η_8	2.34
α_8	0.1907
ν_5	2.43
ν_8	2.79
ν_9	2.885
ν_{11}	3.06
λ_x	2.11×10^{-5} sec^{-1}
λ_{11}	1.665×10^{-19} sec^{-1}
$y_{x,5}$	0.064
$y_{x,8}$	0.06
$y_{x,9}$	0.053
$y_{x,11}$	0.061
$y_{S,5}$	0.01649
$y_{S',8}$	0.03154
$y_{S',9}$	0.03315
$y_{S,11}$	0.035

FIGURE III.2 Logical Flow Diagram for CELL

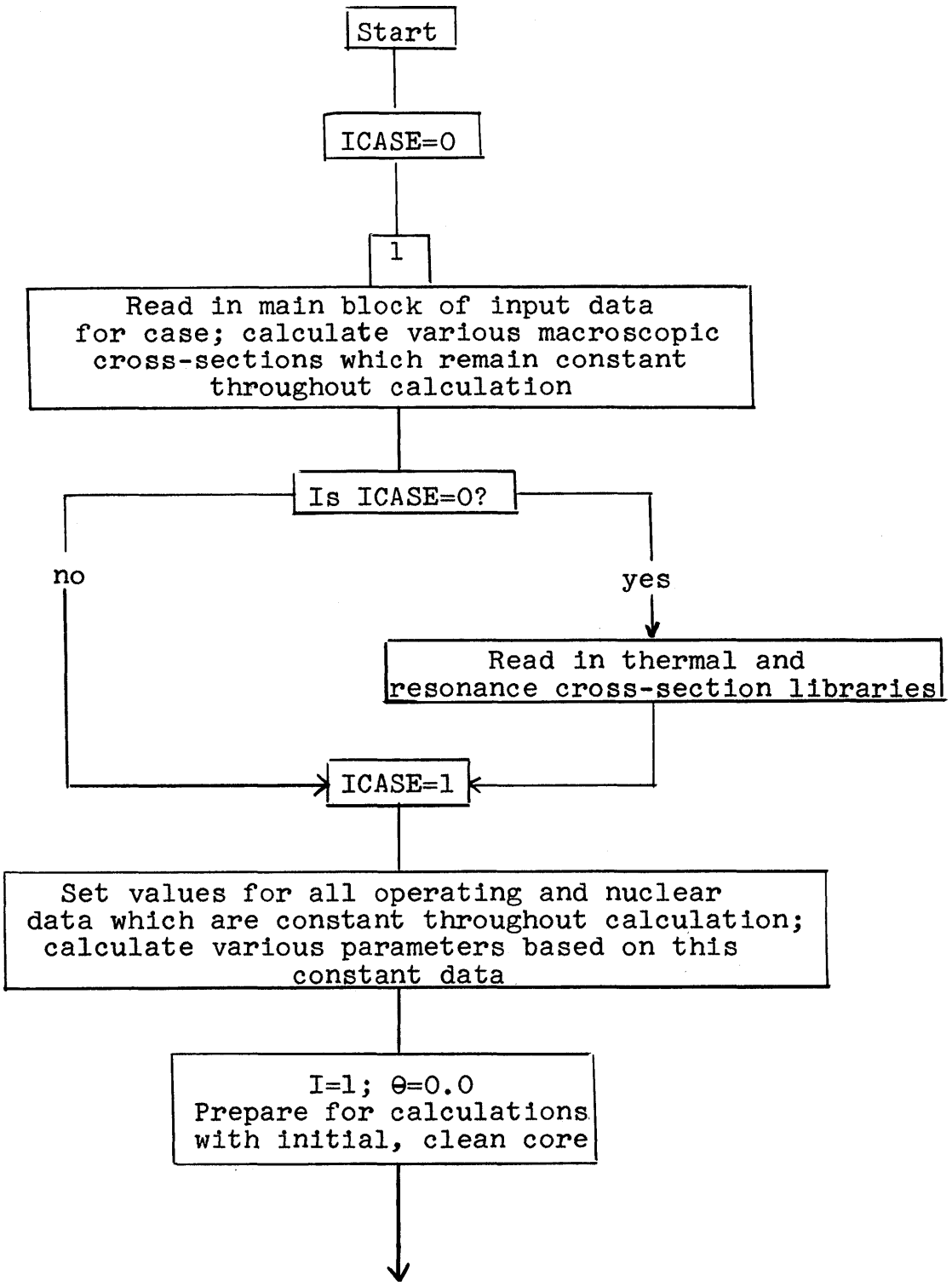

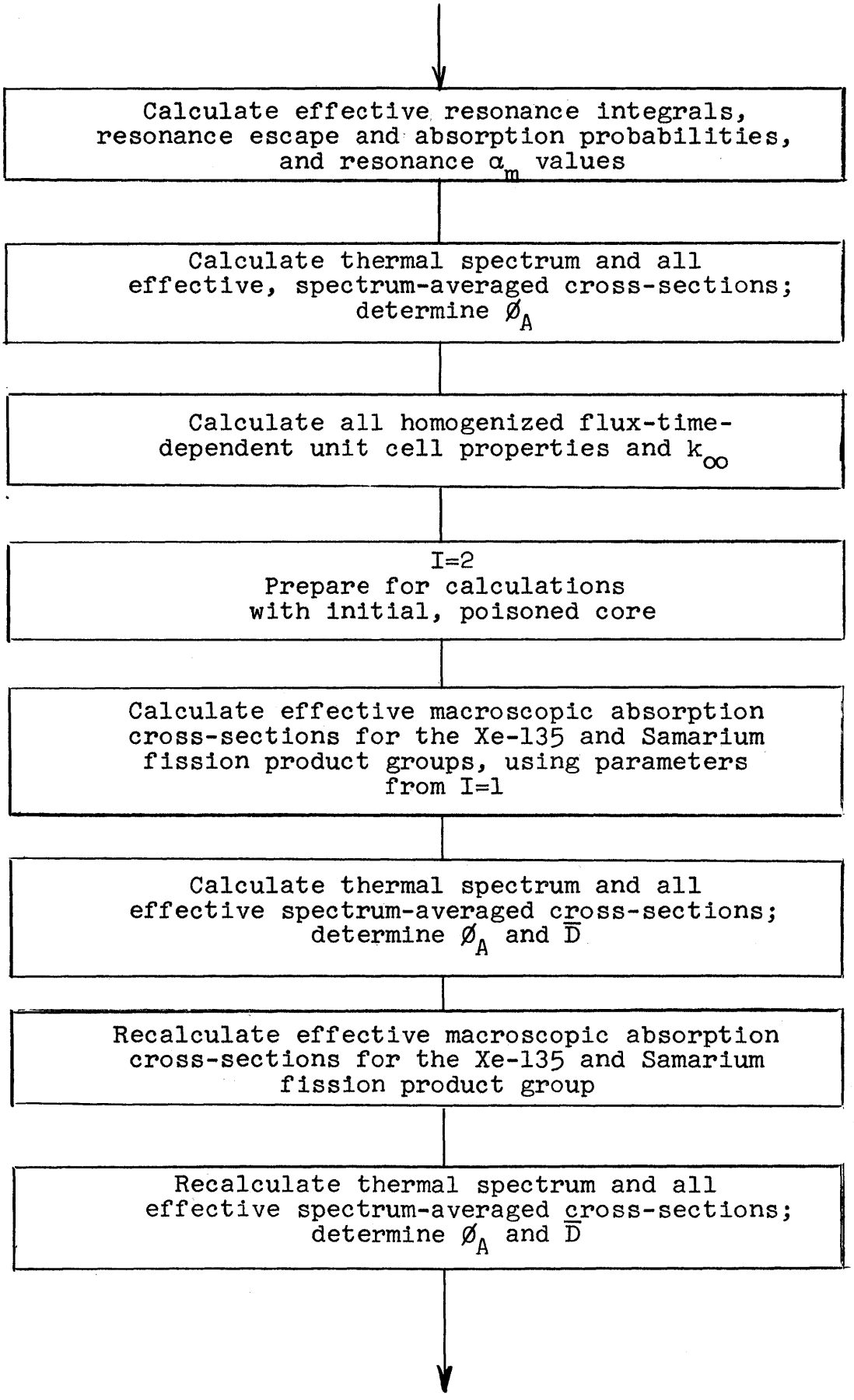
Calculate effective resonance integrals, resonance escape and absorption probabilities, and resonance α_m values
Calculate thermal spectrum and all effective, spectrum-averaged cross-sections; determine ϕ_A
Calculate all homogenized flux-time-dependent unit cell properties and k_∞
I=2
Prepare for calculations with initial, poisoned core
Calculate effective macroscopic absorption cross-sections for the Xe-135 and Samarium fission product groups, using parameters from I=1
Calculate thermal spectrum and all effective spectrum-averaged cross-sections; determine ϕ_A and $\bar{D}$
Recalculate effective macroscopic absorption cross-sections for the Xe-135 and Samarium fission product group
Recalculate thermal spectrum and all effective spectrum-averaged cross-sections; determine ϕ_A and $\bar{D}$

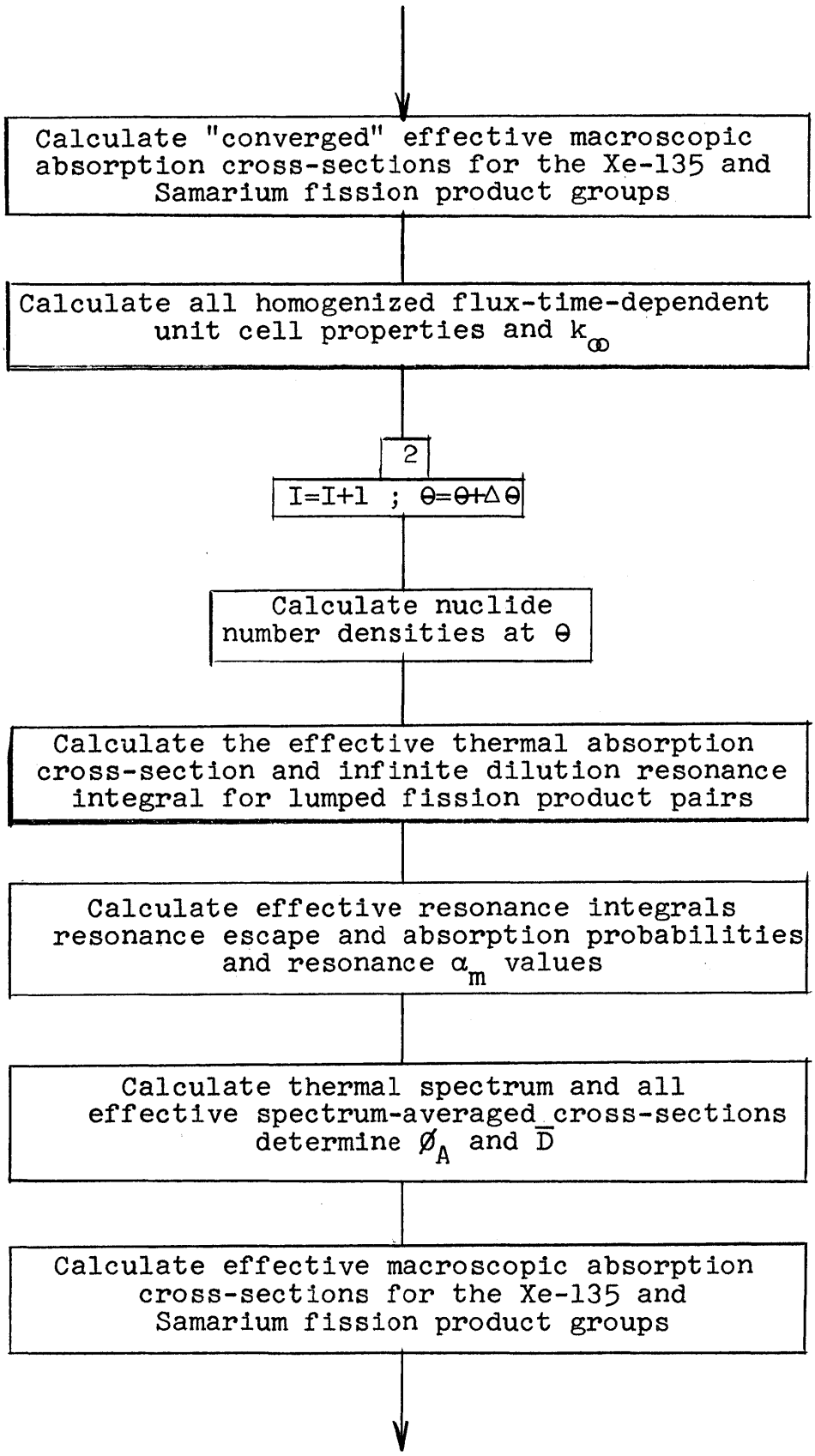
Calculate "converged" effective macroscopic absorption cross-sections for the Xe-135 and Samarium fission product groups
Calculate all homogenized flux-time-dependent unit cell properties and k_∞
2
I=I+1 ; Θ=Θ+ΔΘ
Calculate nuclide number densities at Θ
Calculate the effective thermal absorption cross-section and infinite dilution resonance integral for lumped fission product pairs
Calculate effective resonance integrals resonance escape and absorption probabilities and resonance α_m values
Calculate thermal spectrum and all effective spectrum-averaged cross-sections determine ϕ_A and $\bar{D}$
Calculate effective macroscopic absorption cross-sections for the Xe-135 and Samarium fission product groups

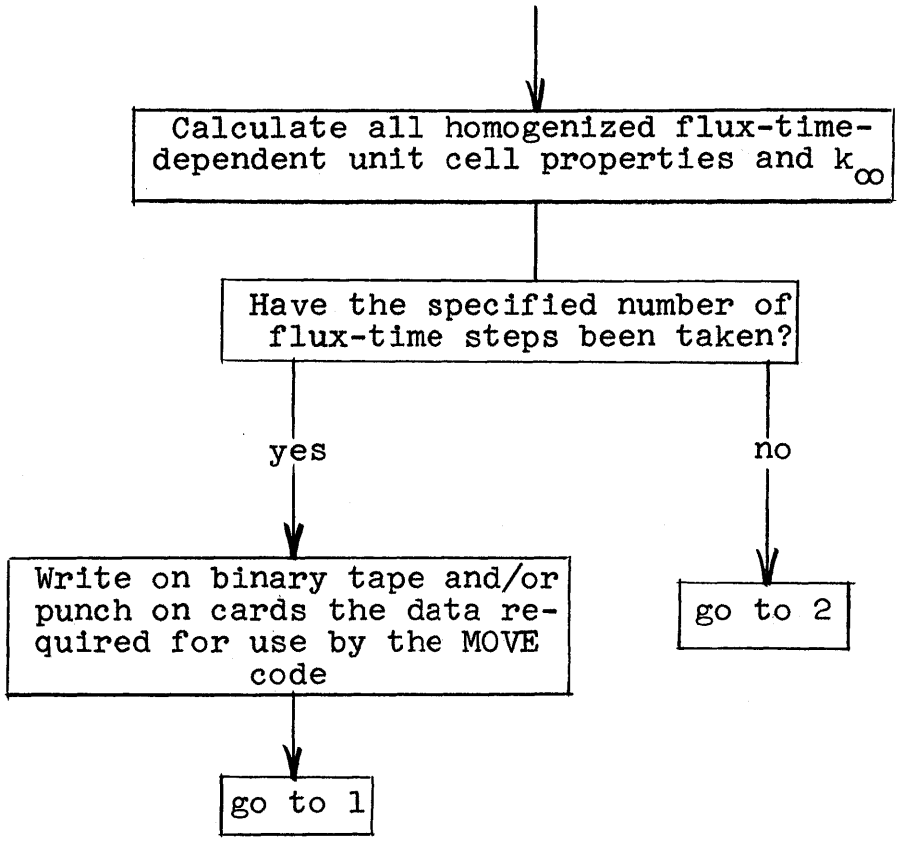
Calculate all homogenized flux-time-dependent unit cell properties and k_∞
Have the specified number of flux-time steps been taken?
yes
no
Write on binary tape and/or punch on cards the data required for use by the MOVE code
go to 2
go to 1

APPENDIX A

NOMENCLATURE

Symbols used on the preceding pages are listed below together with their definitions and, where they differ, with the corresponding symbols used by Beaudreau (5). A dash in the second column indicates that the item was not used in Reference (5). Two major subscripts - i and m - appear with many symbols. Subscript i gives the regional specification, while subscript m denotes the nuclide in question.

Subscripts which may appear in place of i are as follows:

Present Subscript	Reference (5) Subscript	Region Denoted
C	CO	Coolant
CL	CL	Cladding
E	EX	extra
E, ℓ or ℓ	EX - ℓ	Material ℓ in extra region
F	FL or FUEL	Fuel (meat)
FS	FLSUR	Fuel (meat) surface
NF	NF	Composite non-fuel regions
V	VD	Fuel-cladding void

The number of nuclides given below is the same in this work as in Reference (5)

m	Nuclide
5	U-235
6	U-236
7	Lumped fission products (total)
8	U-238

m	Nuclide
9	Pu-239
10	Pu-240
11	Pu-241
12	Pu-242
13	Np-237
14	Lumped fission products from U-238
15	Lumped fission products from U-235
16	Lumped fission products from Pu-239
17	Lumped fission products from Pu-241

The listing of nomenclature follows.

Present Symbol	Reference (5) Symbol	Definition
$A(x)$	$A_{NORM}(x)$	Renormalization factor for thermal disadvantage factors at normalized velocity x
B	--	Fuel exposure, MWD/MT
B^2		Geometric buckling, cm^{-2}
$\overline{D}$		Effective thermal diffusion coefficient for cell, cm
$D(x)$		Thermal diffusion coefficient of the cell at normalized velocity x, cm
E		Neutron energy
E_C		Thermal cutoff energy
E_F	$\overline{E}_{FIS}$	Mean energy of the fission spectrum
E_m	ES_m	Rate of fission energy release in nuclide m per unit thermal flux, MeV/cm
$I_{f,m}$	$RI_{f,m}$	Effective fission resonance integral for nuclide m, barns

Present Symbol	Reference (5) Symbol	Definition
I_i	$RI_{a,2}$	Effective resonance integral for region i, barns
I_m	$RI_{a,m}$	Effective absorption resonance integral for nuclide m, barns
I_7^{∞}	$RI_{FP}^{\infty}(\theta_o)$	Infinite dilution resonance integral for lumped fission products, barns
$I_{8,C}$	$RI_{8,COR}$	Effective resonance integral for U-238 from Strawbridge-Barry correlation, barns
k_{∞}	k_{∞}	Infinite medium multiplication factor
M_m		Mass per gram-mole of nuclide m, grams
N_H		Number density of hydrogen in coolant, atoms/barn-cm
N_i		Number density for region i, molecules/barn-cm
N_m		Number density of nuclide m, atoms/barn-cm
N_m^o		Initial number density of nuclide m, atoms/barn-cm
N_U		Number density of uranium, atoms/barn-cm
p	p_{TOTAL}	Overall resonance escape probability
p_i		Resonance escape probability of region i
p_m		Resonance escape probability of nuclide m
$\overline{P}$	$\overline{PD}$	Average core thermal power density, kw/liter
P_C		Collision probability for resonance neutrons in fuel

Present Symbol	Reference (5) Symbol	Definition
P_1		Fast nonleakage probability
q		Slowing-down density prior to fast leakage, neutrons/cc-sec
R_m	$ENNFIS_m$	Energy released per fission in nuclide m, MeV
S		Surface area of fuel per unit length, cm^2
t		Time variable
T_F	T_{EFF}	Average fuel temperature, ^oK
T_{mod}		Average moderator temperature, ^oK
V		Fuel volume per unit length, cc
V_i		Volume fraction of region i
W(x)		Spectrum-hardening parameter at normalized velocity x
x		Normalized thermal neutron velocity
x_C		Normalized velocity at thermal cutoff energy
y		Resonance scattering parameter, barns
$y_{S,m}$	$y_{Sm,m}$	Samarium group fission yield for nuclide m
$y_{X,m}$	$y_{Xe,m}$	Xe-135 fission yield for nuclide m
Y(x)	$Y_{CELL}(x)$	Thermal flux per unit velocity for the cell at normalized velocity x
$Y_i(x)$		Thermal flux per unit velocity for region i at normalized velocity x

Present Symbol	Reference (5) Symbol	Definition
$\langle 1 - p_m \rangle$		Resonance absorption probability for nuclide m
$\left\langle \frac{1 - p}{1 + \alpha} \right\rangle$		Number of resonance fission per unit of slowing-down density entering resonance region
α_m		Resonance capture-to-fission ratio for nuclide m
γ		Effective resonance shielding factor for the lattice
ϵ		Fast fission effect
η_m		Number of fast neutrons produced per resonance (fast, if U-238) absorption in nuclide m
$\langle \eta(1 - p) \rangle$		Number of neutrons released in resonance fissions per unit of slowing-down density entering resonance region
θ		Thermal flux-time, neutrons/barn
$\Delta\theta$		Thermal flux-time, neutrons/barn
λ_X	λ_{Xe}	Decay constant for Xe-135, sec^{-1}
λ_{11}		Decay constant for Pu-241, sec^{-1}
$\nu\Sigma_f$	$\nu\Sigma_f^{HOM}$	Number of neutrons released by thermal fissions per unit of thermal flux
$\xi\Sigma_S$	$\xi\Sigma_{POT}^{HOM}$	Slowing-down power for cell, cm^{-1}
$(\xi\Sigma_S)_i$	$\xi\Sigma_{POT,i}$	Slowing-down power for region i, cm^{-1}
$\bar{\sigma}_{a,m}$		Effective thermal absorption cross-section for nuclide m, barns
$\sigma_{a,m}(x)$		Absorption cross-section at normalized velocity x for nuclide m, barns
ν_m		Neutrons released per fission in nuclide m

Present Symbol	Reference (5) Symbol	Definition
$\sigma_{a,m}^{res}(E)$	$\sigma_{a,m}^{RES}(E)$	Resonance absorption cross-section at energy E for nuclide m, barns
$\bar{\sigma}_{f,m}$		Effective thermal fission cross-section for nuclide m, barns
$\bar{\sigma}_X$	$\bar{\sigma}_{Xe}$	Effective thermal absorption cross-section for U-238, barns
σ_7	$\sigma_{FP}(\theta_o)$	2200 m/sec absorption cross-section for lumped fission product pairs, barns
$\sigma_{0,8}$	σ_8^{2200}	2200 m/sec absorption cross-section for U-238, barns
$\Sigma(x)$	$\Sigma_{TOT}^{HOM}(x)$	Total cross-section for homogenized cell at normalized velocity x, cm^{-1}
Σ_a	$\Sigma_{TOTAL-Xe}^{HOM}$	Thermal absorption cross-section for homogenized cell excluding Xe-135, cm^{-1}
$\Sigma_a^{res}(E)$	$\Sigma_a^{RES}(E)$	Resonance absorption cross-section for fuel at energy E, cm^{-1}
$\bar{\Sigma}_{a,i}$		Effective thermal absorption cross-section for region i, cm^{-1}
$\Sigma_{a,i}(x)$		Absorption cross-section at normalized velocity x for region i, cm^{-1}
$\Sigma_{a,T}(x)$	$\Sigma_a^{HOM}(x)$	Absorption cross-section at normalized velocity x for homogenized cell including control poison, cm^{-1}
Σ_B	Σ_P^{HOM}	Thermal absorption cross-section for control poison homogenized over cell, cm^{-1}
$\Sigma_B(x)$	$\Sigma_{POISON}^{HOM}(x)$	Absorption cross-section at normalized velocity x for control poison homogenized over cell, cm^{-1}

Present Symbol	Reference (5) Symbol	Definition
Σ_f	Σ_f^{HOM}	Thermal fission cross-section for homogenized cell, cm^{-1}
$\overline{\Sigma}_{FP}$		Effective thermal absorption cross-section for lumped fission products, cm^{-1}
Σ_{PC}	$\Sigma_{POT,FLMOD}$	Resonance potential scattering cross-section of low-atomic-weight atoms contained in fuel molecules, cm^{-1}
Σ_{PT}	$\Sigma_{POT,FLTOT}$	Resonance potential scattering cross-section of fuel molecules, cm^{-1}
$\overline{\Sigma}_{Sm}$	Σ_{Sm}	Equilibrium effective thermal absorption cross-section for Samarium fission product group, cm^{-1}
$\Sigma_{TR}(x)$	$\Sigma_{TR}^{HOM}(x)$	Transport-corrected scattering cross-section at normalized velocity x for homogenized cell, cm^{-1}
$\Sigma_{TR,i}$		Transport-corrected thermal scattering cross-section for region i, cm^{-1}
Σ_X		Thermal absorption cross-section for equilibrium Xe-135 homogenized over cell, cm^{-1}
$\Sigma_{X,M}$	$\Sigma_{MAX\ Xe}^{HOM}$	Thermal absorption cross-section for equilibrium Xe-135, neglecting Xe-135 decay, homogenized over cell, cm^{-1}
$\overline{\Sigma}_{X,M}$	$\Sigma_{MAX\ Xe}$	Effective thermal absorption cross-section for equilibrium Xe-135, neglecting Xe-135 decay, cm^{-1}
$\Sigma_{0,i}$	$\Sigma_{2200,i}$	2200 m/sec absorption cross-section for region i, cm^{-1}
ϕ	ϕ_{CELL}	Integrated thermal flux for cell in relative units.
$\overline{\Sigma}_X$	Σ_{Xe}	Effective thermal absorption cross-section for equilibrium Xe-135, cm^{-1}

Present Symbol	Reference (5) Symbol	Definition
ϕ_A	$\overline{\Phi}_{CELL}$	Absolute magnitude of integrated thermal flux for cell, n/cm^2-sec
ϕ_E/ϕ_C	ϕ_{EX}/ϕ_{CO}	Ratio of average thermal flux in extra region to average thermal flux in coolant
(ϕ_E/ϕ_C)	ϕ_{EX-}/ϕ_{CO}	Ratio of thermal flux in extra region material to average thermal flux in coolant
ψ	DANC	Resonance blackness of nonfuel portion of lattice

APPENDIX B

REFERENCES

1. R. T. Shanstrom, M. Benedict, and C. T. McDaniel, "Fuel Cycles in Nuclear Reactors," NYO-2131 (1959).

2. N. B. McLeod, et al., "The Effect of Fuel and Poison Management on Nuclear Power Systems," NYO-9715 (1961).

3. P. F. Menezes, "Comparison of Observed and Predicted Performance of the First Core of the Yankee Reactor," MIT, SM thesis in Nuclear Engineering (September, 1964).

4. D. A. Goellner, "The Effect of Uranium-236 and Neptunium-237 on the Value of Uranium as Feed for Pressurized Water Reactors," MIT, Ph.D. thesis in Nuclear Engineering (October, 1967).

5. J. J. Beaudreau, "Development and Evaluation of the Point Depletion Code CELL," MIT, SM thesis in Nuclear Engineering (June, 1967).

6. J. E. Wilkins, "Effect of the Temperature of the Moderator on the Velocity Distribution of Neutrons for a Heavy Moderator", CP-2481 (1944).

7. E. P. Wigner and J. E. Wilkins, Jr., "Effect of the Temperature of the Moderator on the Velocity Distribution of Neutrons with Numerical Calculations for H as the Moderator," AECD-2275 (1944).

8. H. Amster and R. Suarez, "The Calculation of Thermal Constants Averaged over a Wigner-Wilkins Flux Spectrum: Description of the SOFOCATE Code," WAPD-TM-39 (1957).

9. R. F. Barry, "LEOPARD - A Spectrum Dependent Non-Spatial Depletion Code for the IBM-7094," WCAP-3269-26 (1963).

10. C. H. Westcott, "Effective Cross-Section Values for Well-Moderated Thermal Reactor Spectra," AECL-1101, 3rd ed. (1962).

11. R. L. Crowther and J. W. Weil, "The Effective Cross-Section of Pu-240 in Long Term Reactivity Calculations," GEAP-2058.

12. "San Onofre Nuclear Generating Station - Reference Core Design," WCAP-3269-7 (1965).

13. H. W. Graves, Jr., Personal communication to M. Benedict (March, 1965).

14. L. E. Strawbridge and R. F. Barry, "Criticality Calculations for Uniform Water-Moderated Lattices," Nuclear Science and Engineering, 23 (1), 58-73 (1965).

15. A. Amouyal, P. Benoist, and J. Horowitz, "Nouvelle Methode de Determination du Facteur D'Utilisation Thermique D'Une Cellule," Journal of Nuclear Energy, 6, 79-98 (1957).

16. D. G. Hurst, "Calculated Cross-Sections of Irradiation Fission Products," CRRP-659, (AECL-346) (1956).

17. J. R. Lamarsh, Introduction to Nuclear Reactor Theory, Addison-Wesley Publishing Company, Inc., Reading, Mass. (1966).

18. A. Sauer, "Approximate Escape Probabilities," Nuclear Science and Engineering, 16 (3), 329-335 (1963).

19. D. Klein, et al., "Measurements of Thermal Utilization, Resonance Escape Probability, and Fast Effect in Water-Moderated, Slightly Enriched Uranium and Uranium Oxide Lattices," Nuclear Science and Engineering, 3, 395-402 (1958).

20. D. B. Wehmeyer, "Analysis of Water-Moderated UO_2 and ThO_2 Lattices," Panel on Light Water Lattices, No. 12 of IAEA Technical Reports Series, Vienna (1962).

21. M. J. Romanelli, "Runge-Kutta Methods for the Solution of Ordinary Differential Equations," in Mathematical Methods for Digital Computers, pp. 110-120, Wiley and Sons (1960).